2021 Fall

"Phase Transformation *in* Materials"

12.01.2021

Eun Soo Park

Office: 33-313
Telephone: 880-7221
Email: espark@snu.ac.kr
Office hours: by an appointment

5. Diffusion Transformations in solid

: diffusional nucleation & growth

(a) Precipitation

$$\alpha' \rightarrow \alpha + \beta$$

Metastable supersaturated
Solid solution

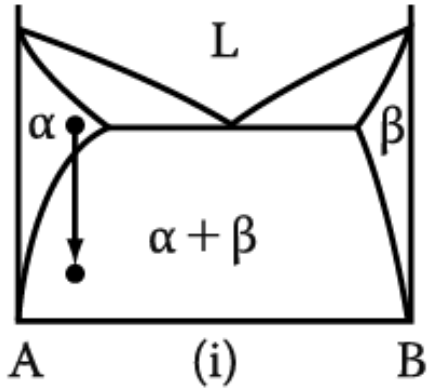

Homogeneous Nucleation

$$\Delta G = -V\Delta G_V + A\gamma + V\Delta G_S$$

Heterogeneous Nucleation

$$\Delta G_{het} = -V(\Delta G_V - \Delta G_S) + A\gamma - \Delta G_d$$

$$N_{\text{hom}} = \omega C_0 \exp\left(-\frac{\Delta G_m}{kT}\right)\exp\left(-\frac{\Delta G^*}{kT}\right)$$

➡ suitable nucleation sites ~ nonequilibrium defects
(creation of nucleus~destruction of a defect($-\Delta G_d$))

(b) Eutectoid Transformation

Composition of product phases differs from that of a parent phase.
→ long-range diffusion

Which transformation proceeds by short-range diffusion?

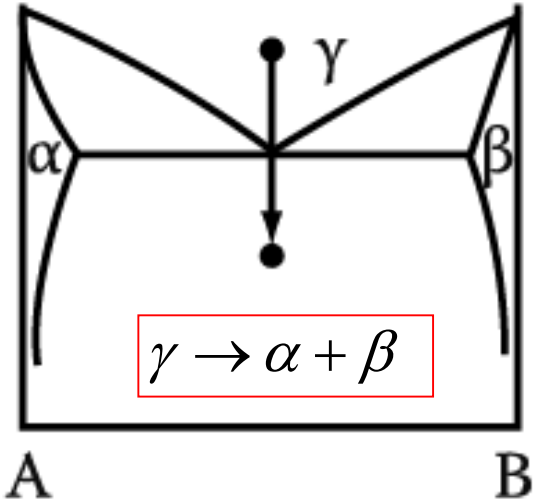

5. Diffusion Transformations in solid

(c) Order-Disorder Transformation

$$\alpha \rightarrow \alpha'$$

Disorder (high temp.) Order (low temp.)

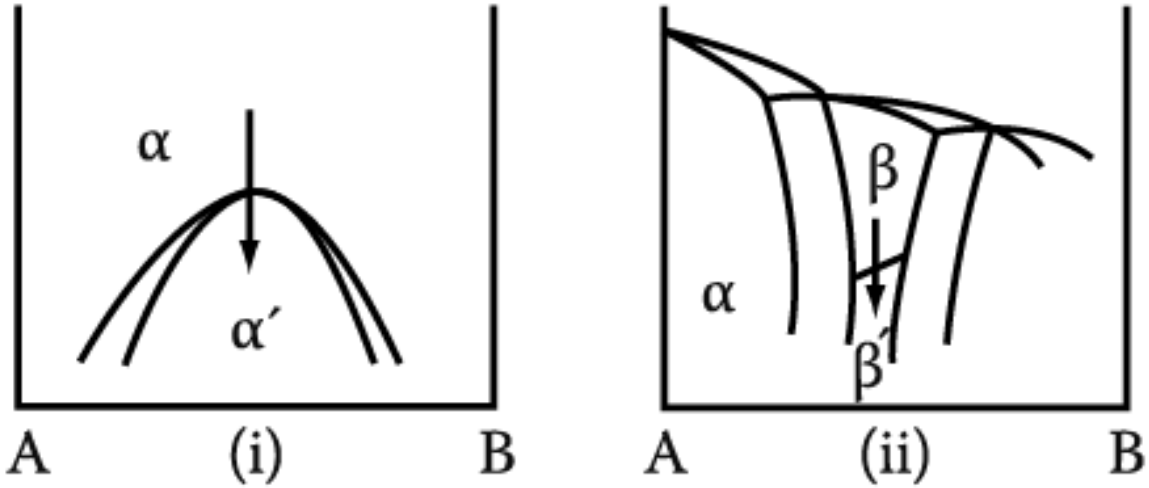

(d) Massive Transformation

: The original phase decomposes into one or more new phases which have the same composition as the parent phase, but different crystal structures.

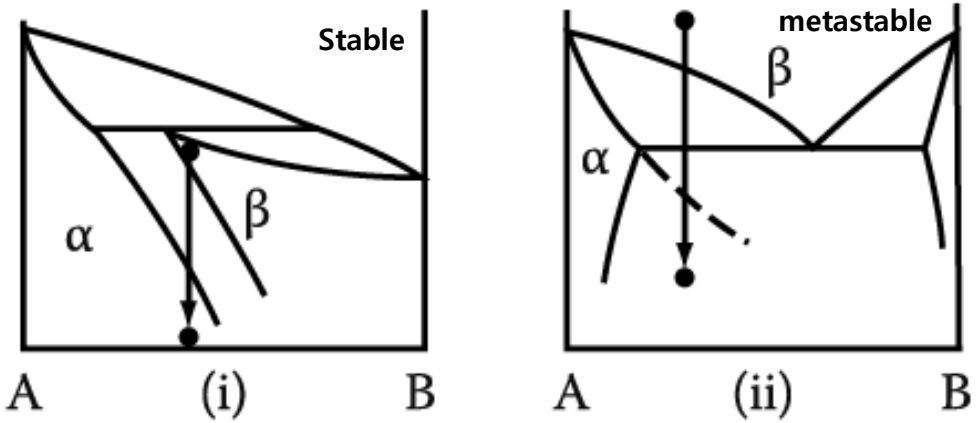

$$\beta \rightarrow \alpha$$

(e) Polymorphic Transformation

In single component systems, different crystal structures are stable over different temper-ature ranges.

5.6. The Precipitation of Ferrite from Austenite (γ→α)

(Most important nucleation site: Grain boundary and the surface of inclusions)

The Iron-Carbon Phase Diagram

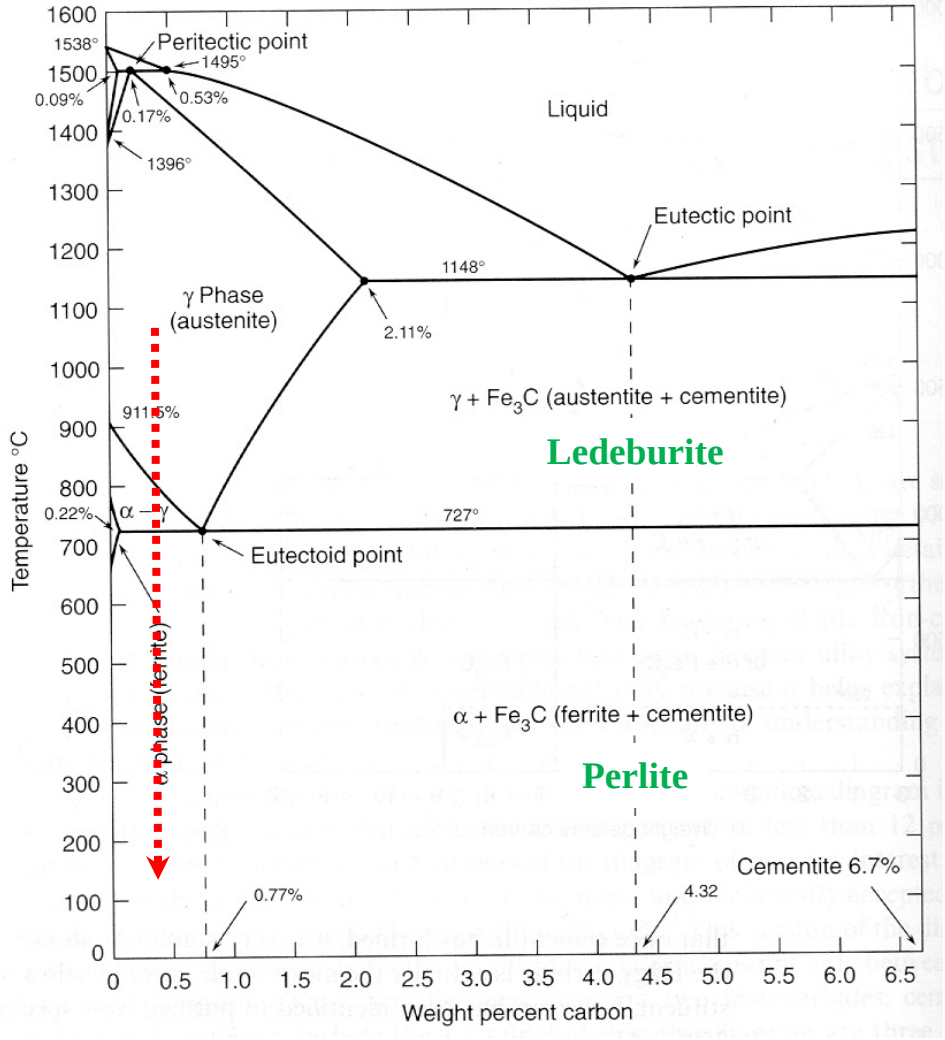

Microstructure (0.4 wt%C) evolved by slow cooling (air, furnace) ?

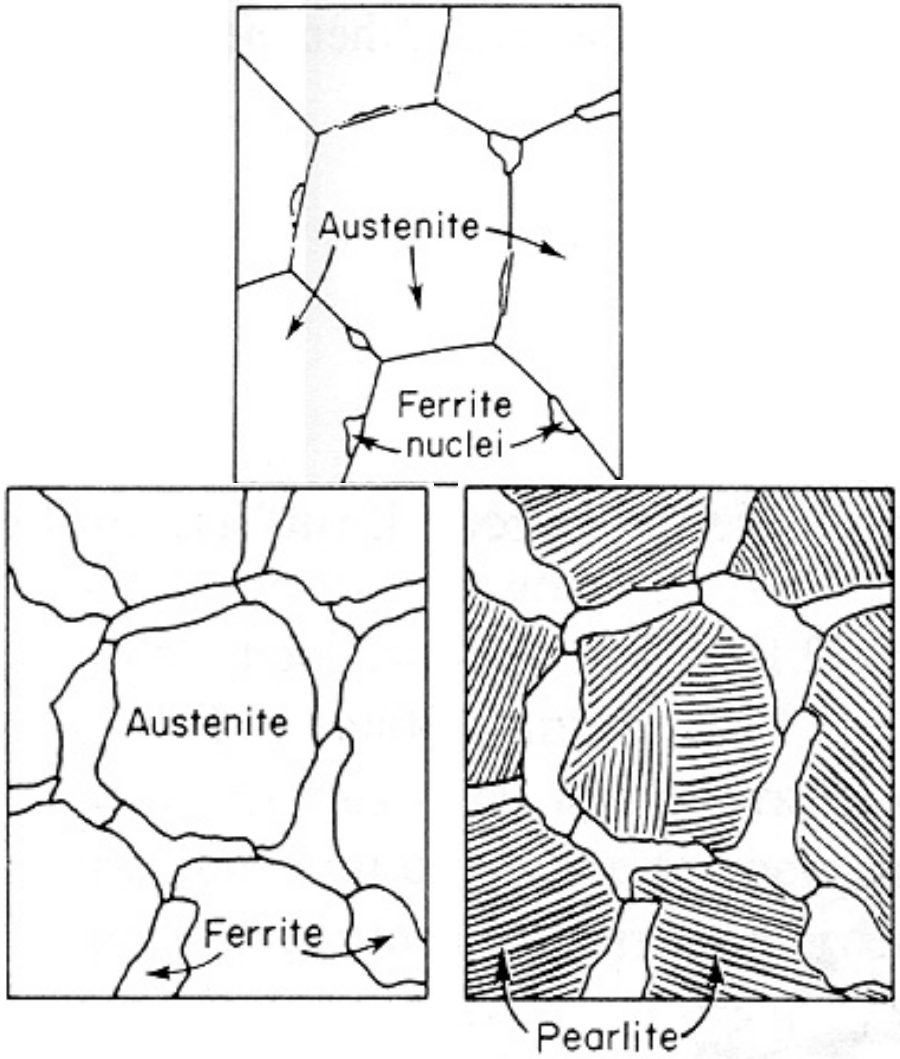

5.6. The Precipitation of Ferrite from Austenite

Diffusional Transformation of Austenite into Ferrite

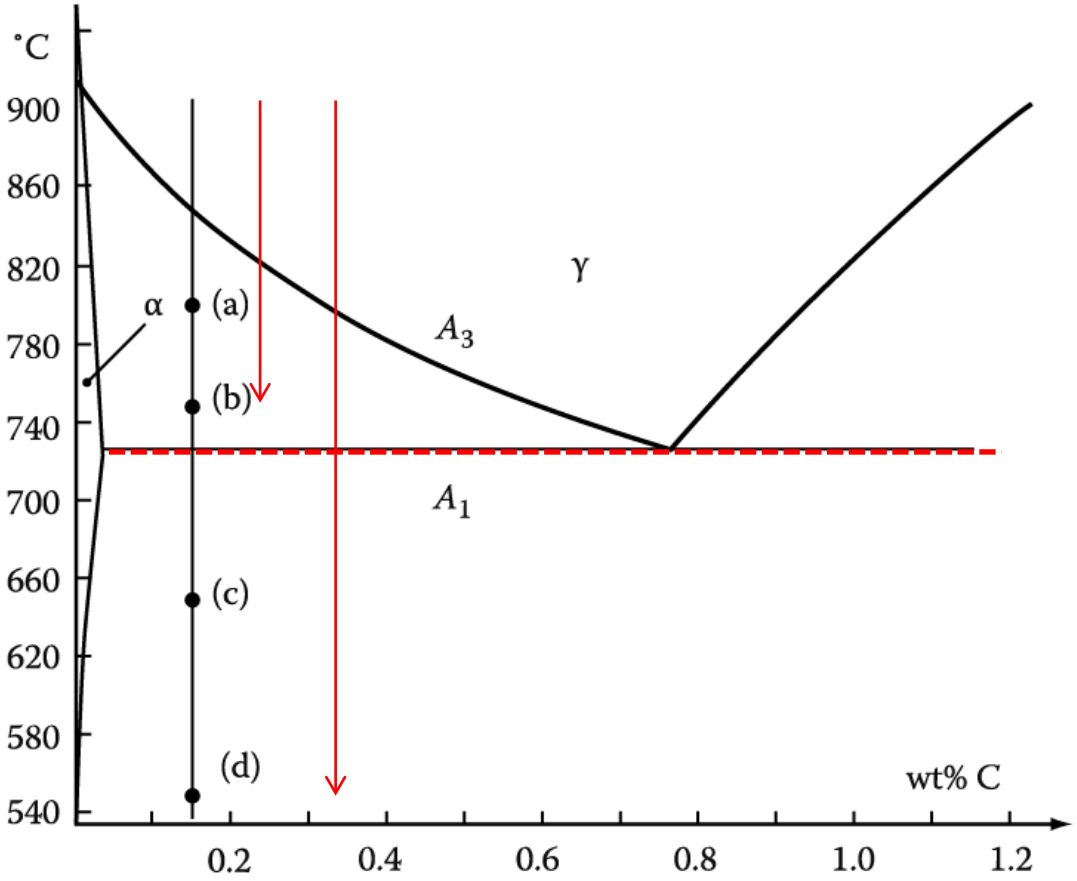

Figure 5.45 Holding temperature for steel in Figure. 5.46

Fe-0.15 wt%C

After being austenitized, held at

(a) 800°C for 150 s

(b) 750°C for 40 s

(c) 650°C for 9 s

(d) 550°C for 2 s and

then quenched to room T.

What would be the microstructures?

* Massive, Martensite Transformation

Martensite

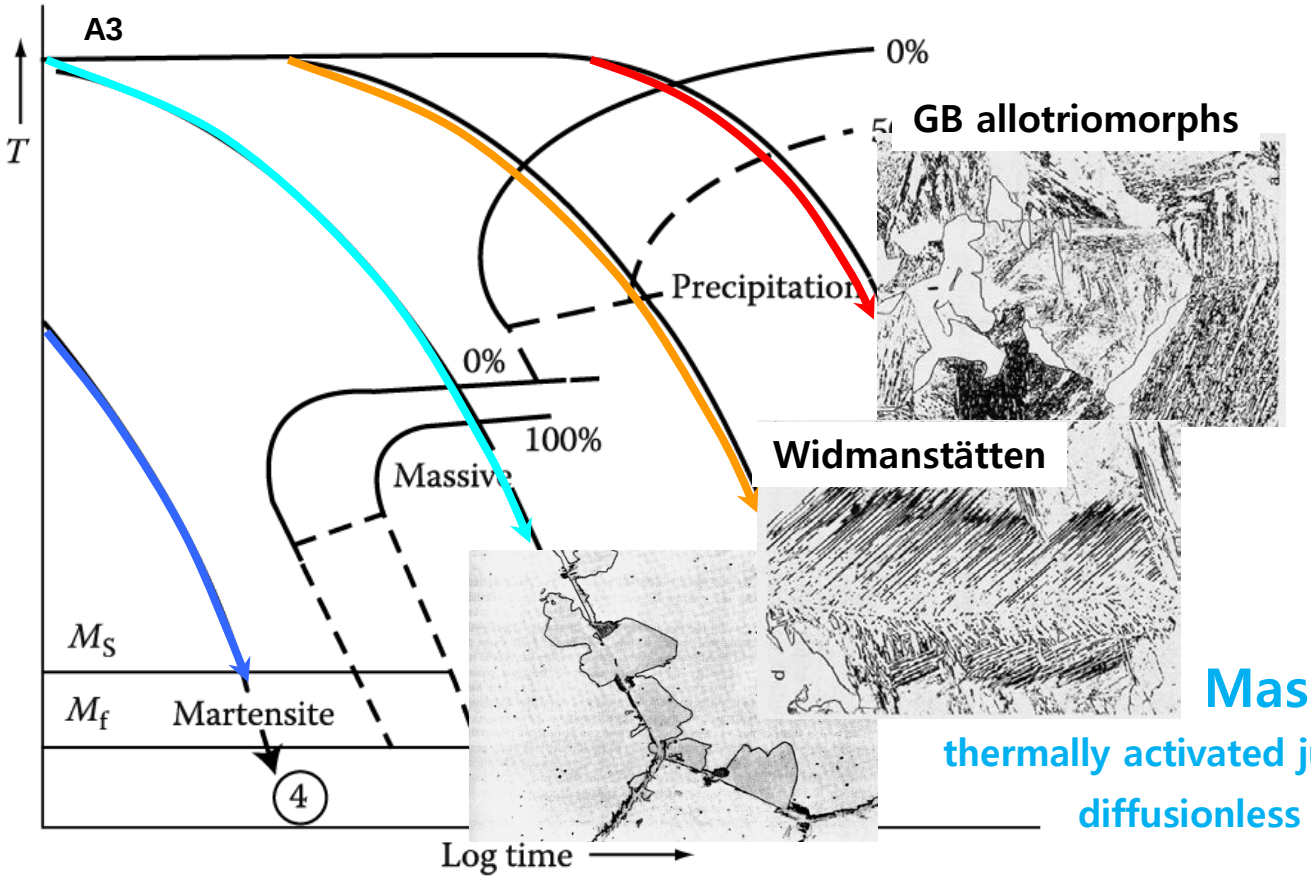

GB allotriomorphs

Widmanstätten

Massive Transformation

thermally activated jumping across the α/β interface

diffusionless civilian transformation

β is sheared into α by the cooperative move-ment of atoms across a glissile interface

diffusionless military transformation

Martensite Transformation

Fig. 5.75 A possible CCT diagram for systems showing a massive transformation. Slow cooling (1) produces equiaxed α. Widmanstatten morphologies result from faster cooling (2). Moderately rapid quenching (3) produces the massive transformation, while the highest quench rate (4) leads to a martensitic transformation.

Growth of Pearlite: analogous to the growth of a lamellar eutectic

Min. possible: (S*) $\propto 1/\Delta T$ / Growth rate : mainly lattice diffusion $v = kD_c^{\gamma}(\Delta T)^2$

Interlamellar spacing of pearlite colonies mainly boundary diffusion $v = kD_b(\Delta T)^3$

Relative Positions of the Transformation curves for Pearlite and Bainite in Plain Carbon Eutectoid Steels.

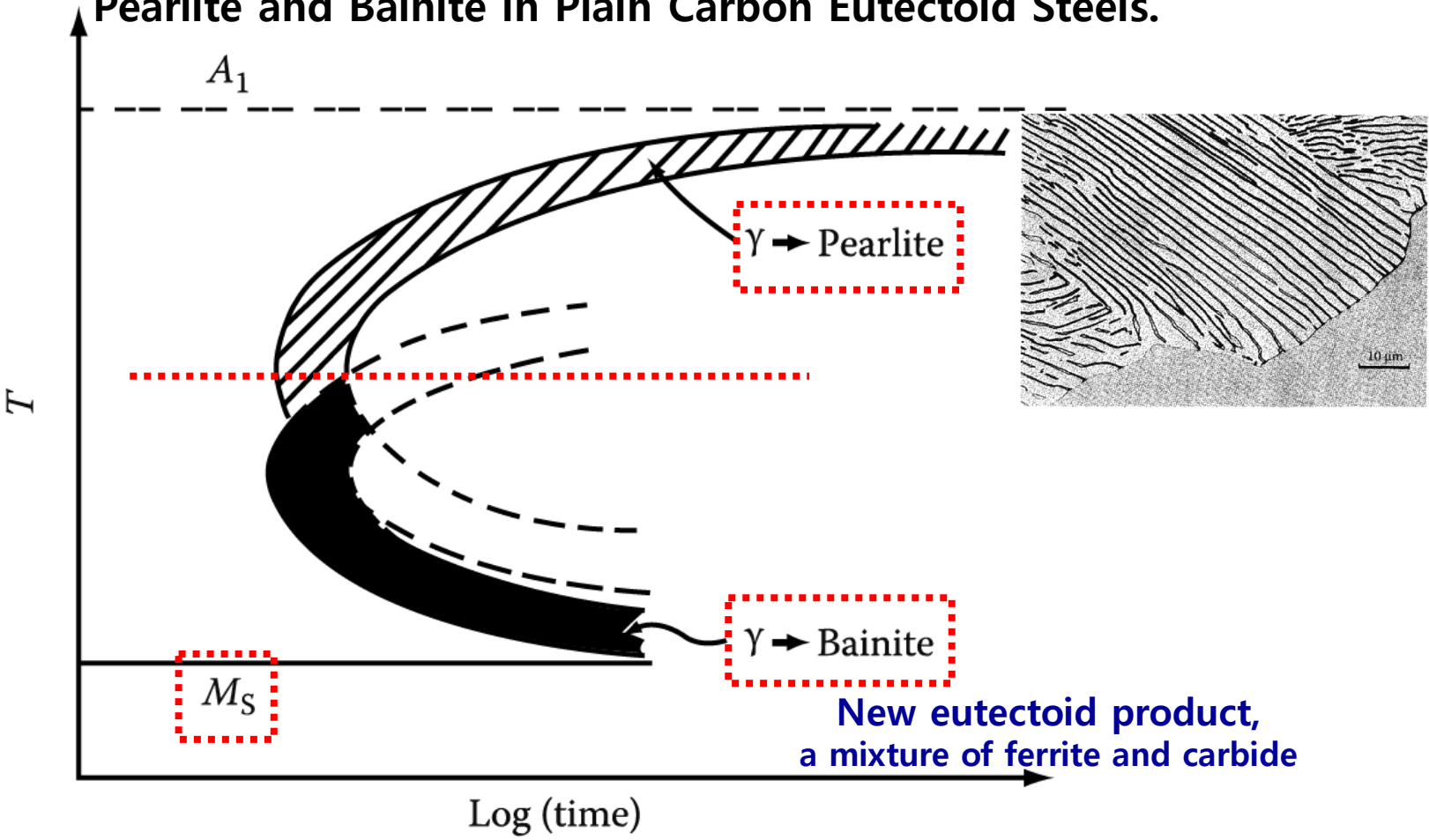

Figure 5.64 Schematic diagram showing relative positions of the transformation curves for pearlite and bainite in plain carbon eutectoid steel.

For alloys of different carbon content, A_3 and T_w vary and show parallel manner each other.

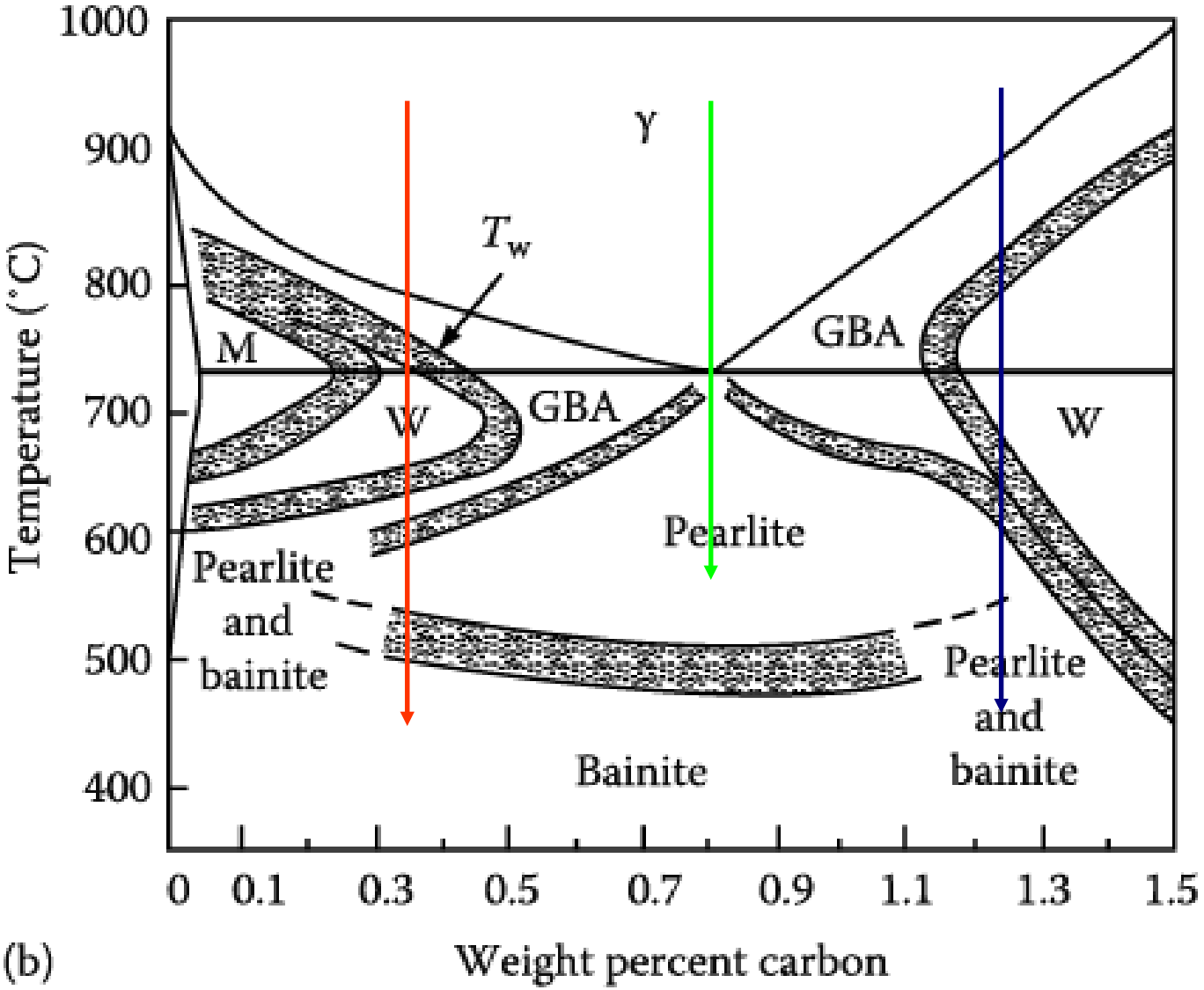

(GBA: GB allotriomorphs, W: Widmanstatten sideplates/intermolecular plates, M: Massive ferrite)

Figure 5.48 (b) Temperature-composition regions in which the various morphologies are dominant at late reaction times in specimens with ASTM grain size Nos. 0-1.

Contents in Phase Transformation

Background to understand phase transformation

- (Ch1) Thermodynamics and Phase Diagrams
- (Ch2) Diffusion: Kinetics
- (Ch3) Crystal Interface and Microstructure

Representative Phase transformation

- (Ch4) Solidification: Liquid → Solid
- (Ch5) Diffusional Transformations in Solid: Solid → Solid
- (Ch6) Diffusionless Transformations: Solid → Solid

Contents for today's class

< Phase Transformation in Solids >

2) Diffusionless Transformation

Q1: What is a martensitic transformation?

Q2: Microstructural characteristics of martensite?

Q3: Driving Forces of Martensitic transformation?

Q4: Why tetragonal Fe-C martensite?

Q5: Martensite crystallography (Orientation btw M & γ)

Q6: Mechanisms for martensitic transformations?

Q1: What is a martensitic transformation?

One of the most important technological processes is the **hardening of steel by quenching**.

Chapter 6 Diffusionless Transformation

Individual atomic movements are less than one interatomic spacing.

→ Martensite Transformation

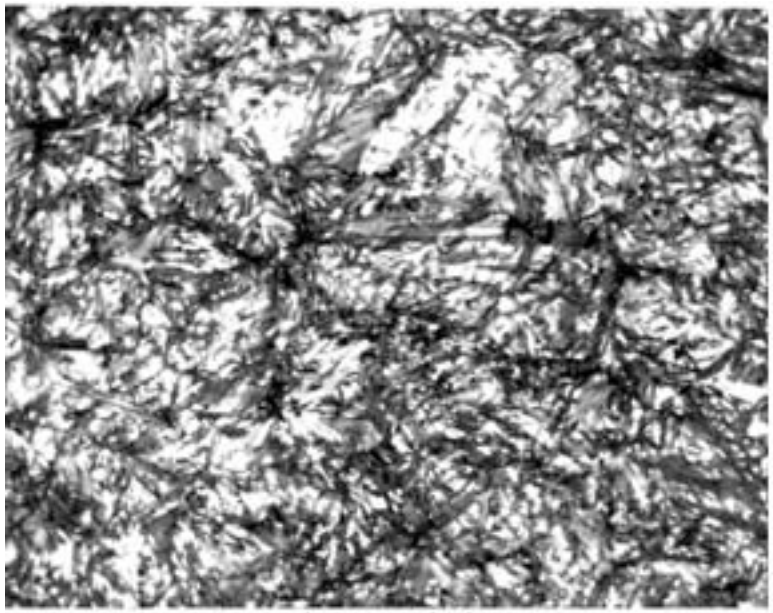

(γ→α) Martensite with some retained austenite

"Needle like" Structure of martensite

Supersaturated solid solution of carbon in α-Fe

Named for the German metallurgist Adolph Martens, Martensite is the hardened phase of steel that is obtained by cooling Austenite fast enough to trap carbon atoms within the cubic iron matrix distorting it into a body centered tetragonal structure. Now, martensite is used in physical metallurgy to describe any diffusionless trans. product.

Military Transformations

- **What is a martensitic transformation?**

  Most phase transformations studied in this course have been diffusional transformations where long range diffusion is required for the (nucleation and) growth of the new phase(s).

- **There is a whole other class of *military transformations* which are *diffusionless transformations* in which the atoms move only short distances (less than one interatomic spacing) in order to join the new phase.**

- **These transformations are *also* subject to the constraints of nucleation and growth. They are (almost invariably) associated with allotropic transformations (동소변태).**

Classification of Transformations

	Civilian	Military
Diffusion Required	**Precipitation, Spinodal Decomposition**	**?**
Diffusionless	**Massive Transformations**	**Martensitic Transformations**

Massive vs. Martensitic Transformations

- There are two basic types of *diffusionless* transformations.
- One is the ***massive transformation***. In this type, a diffusionless transformation takes place ① without a definite orientation relationship. The interphase boundary (between parent and product phases) migrates so as to allow the new phase to grow. It is, however, a ② civilian transformation because the atoms move individually.

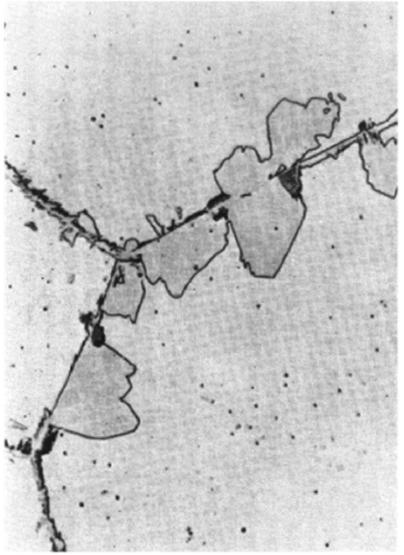

- The other is the ***martensitic transformation***. In this type, the change in phase involves a ① definite orientation relationship because the atoms have to ② move in a coordinated manner. (Military transformation) There is always a ③ change in shape which means that there is a strain associated with the transformation.

Microstructure of Martensite

- The microstructural characteristics of martensite are:
  - **the product (martensite) phase has a well defined crystallographic relationship with the parent (matrix).**

1) martensite(designated α') forms as platelets within grains.

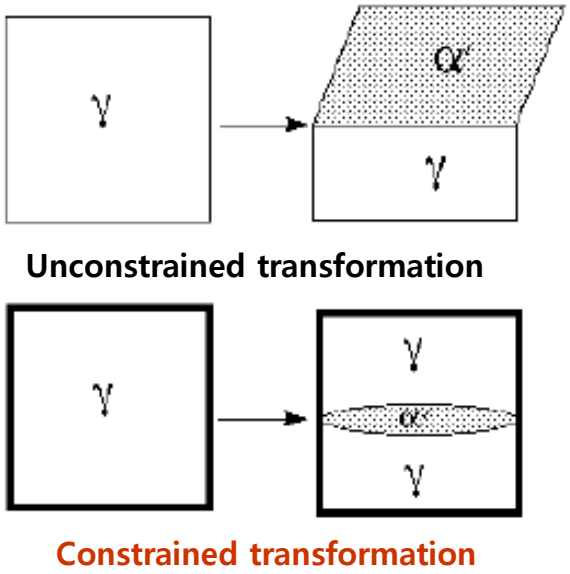

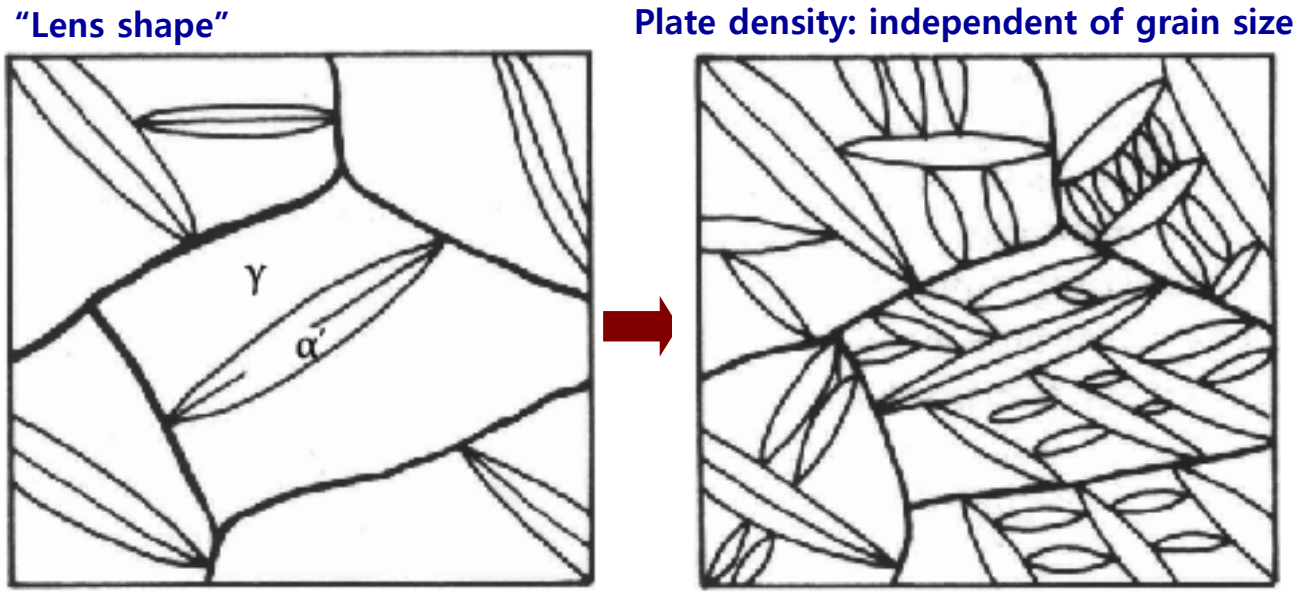

Fig. 6.1 Growth of martensite with increasing cooling below Ms.

→ Martensite formation rarely goes to completion

Microstructure of Martensite

- The microstructural characteristics of martensite are:

2) each platelet is accompanied by a shape change.

- the shape change appears to be a simple shear parallel to a habit plane (the common, coherent plane between the phases) and a "uniaxial expansion (dilatation) normal to the habit plane".

strain associated with the transformation

Polished surface_elastic deformation or tilting
→ but, remain continuous after the transformation

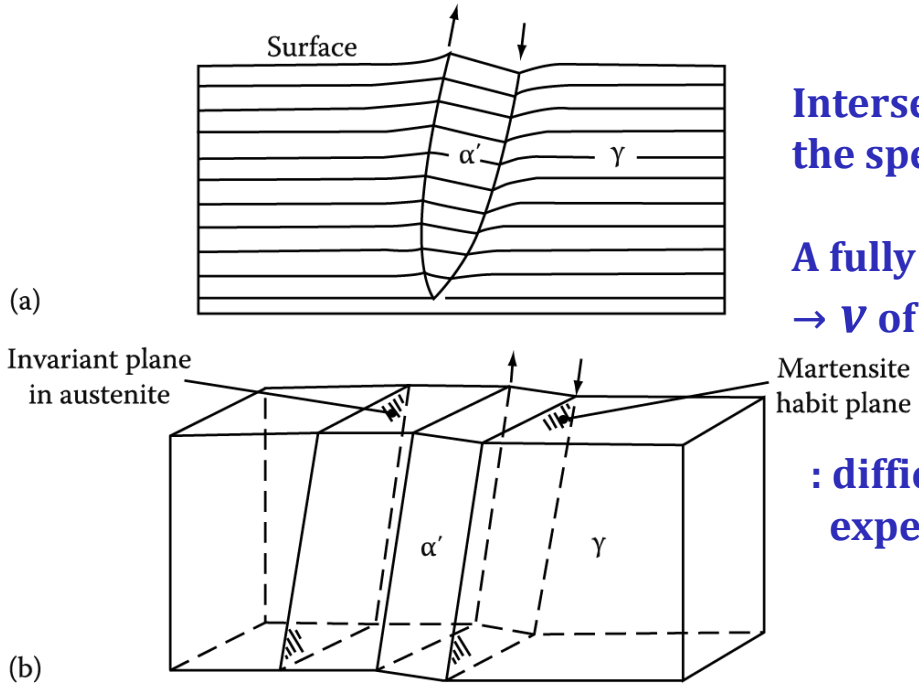

Intersection of the lenses with the surface of the specimen does not result in any discontinuity.

A fully grown plate spanning a whole grain ~10^{-7} sec
→ v of α′/γ interface∝ speed of sound in solid

: difficult process to study M nucleation and growth experimentally

Fig. 6.2 Illustrating how a martensite plate remains macroscopically coherent with the surrounding austenite and even the surface it intersects.

Microstructures

M_f temperature (M finish) corresponds to that temperature below which further cooling does not increase the amount of M.
→ 10-15% retained γ: common feature of higher C content alloys

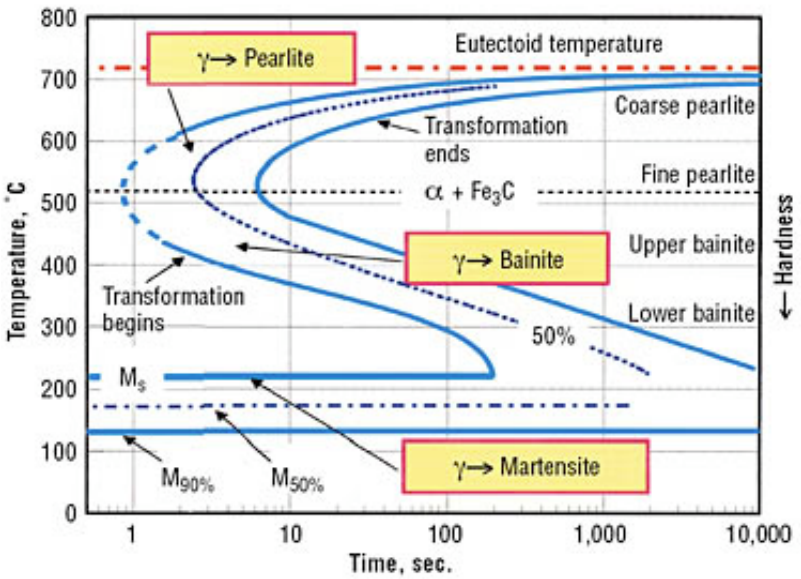

Low C (lath)

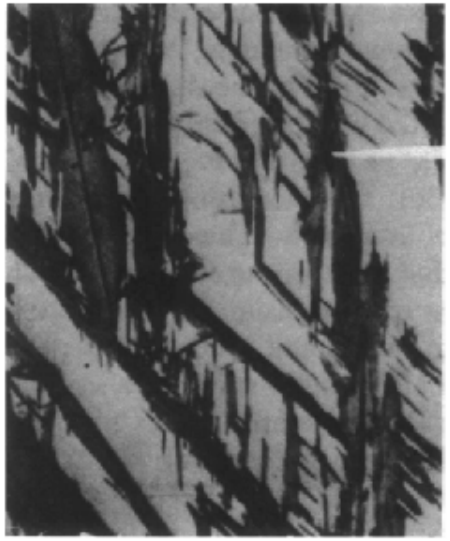

Medium C (plate)

Fe-Ni (plate, some isothermal growth)

Fig. 6.1 (c-e) Different martensite morphologies in iron alloys

Control of Mechanical Properties By Proper Heat Treatment in Iron-Carbon Alloy

Proper heat treatment (tempering)

Martensite

- Tip of needle shape grain
- Nucleation site of fracture
- Brittle

Tempered martensite

- Very small & spherical shape grain
- Good strength, ductility, toughness

Q3:

Driving Forces of Martensitic transformation

- These transformations require ***larger driving forces*** than for diffusional transformations. **(= large undercooling, ΔT)**

- Why? In order for a transformation to occur without long range diffusion, it must take place ***without a change in composition***.

- This leads to the so-called T_0 **concept**, which is the temperature at which the new phase can appear with **a net decrease in free energy** *at the same composition as the parent (matrix) phase*.

- As the following diagram demonstrates, the temperature, T_0, at which segregation-less transformation becomes possible (i.e. a decrease in free energy would occur), is always less than the liquidus temperature.

Free Energy - Composition: T_0

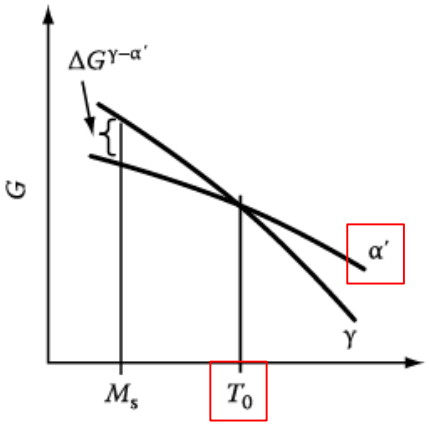

α *product*

T_1

$\Delta G^{\gamma \rightarrow \alpha}$

γ *parent*

Common tangent

G

$\Delta G^{\gamma \rightarrow \alpha'}$

T_2

$T_1 > T_2$

X

Diffusionless transformation *impossible* at T_1,

Diffusionless transformation *possible* at T_2;

T_2 corresponds to figure 6.3b in P&E.

"T_0" is defined by no difference in free energy between the phases, $\Delta G=0$.

Driving Force Estimation

- The driving force for a martensitic transformation can be estimated in exactly the same way as for other transformations such as solidification.

- Provided that an enthalpy (latent heat of transformation) is known for the transformation, the driving force can be estimated as proportional to **the latent heat** and **the undercooling below T_0**.

$$\Delta G = \frac{L\Delta T}{T_m} \Rightarrow \Delta G^{\gamma\rightarrow\alpha'} = \Delta H^{\gamma\rightarrow\alpha'}\Delta T/T_0 = \Delta H^{\gamma\rightarrow\alpha'}\frac{(T_0 - M_S)}{T_0}$$

Alloy	$\Delta H^{\gamma\rightarrow\alpha'}$ (J mol^{-1})	$T_0 - M_s$(K)	$-\Delta G^{\gamma\rightarrow\alpha'}$ (J mol^{-1})
Ti–Ni	1550	20	92
Cu–Al	170–270	20–60	19.3 ± 7.6
Au–Cd	290	10	11.8
Fe–Ni 28%	1930	140	840
Fe–C			1260
Fe–Pt 24%	340	10	17
Ordered			
Fe–Pt	2390	~150	~1260
Disordered			

* Large differences in $\Delta G^{\gamma\rightarrow\alpha'}$ btw disordered and ordered alloys (a relatively small ΔT)

Source: From Guénin, G., PhD thesis, Polytechnical Institute of Lyon, 1979.

Table 6.1. Comparisons of Calorimetric Measurements of Enthalpy and Undercooling in some M alloys

Various ways of
showing the martensite transformation

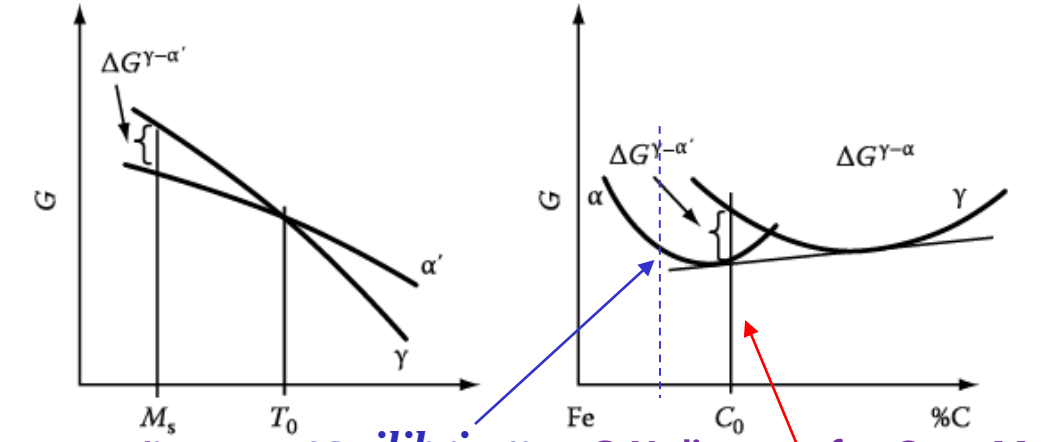

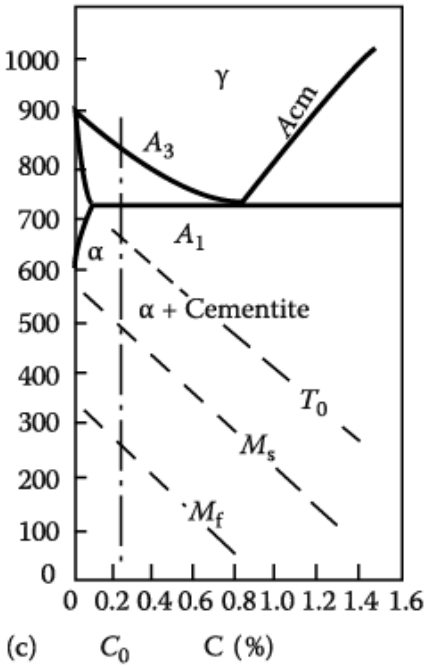

Fe-C phase diagram
Variation of $T_0/M_s/M_f$

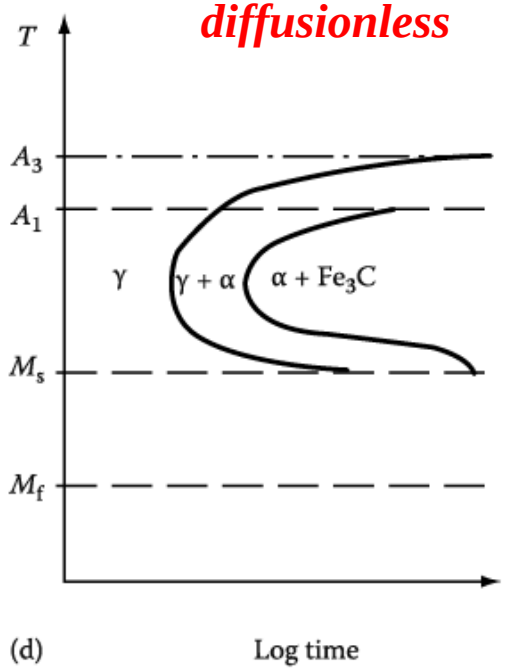

TTT diagram
for alloy C_0 in (c)

Note that the M_s line is horizontal in the TTT diagram; also, the M_f line.

Some retained austenite can be left even below M_f. In particular, as much as 10%-15% retained austenite is a common feature of especially the higher C content alloys such as those used for ball bearing steels.

Q4: Why tetragonal Fe-C martensite?

6.1.1 Solid Solution of carbon in Iron (철의 탄소고용체)

Figure 6.4 Illustrating possible sites for interstitial atoms in the fcc or hcp lattices.

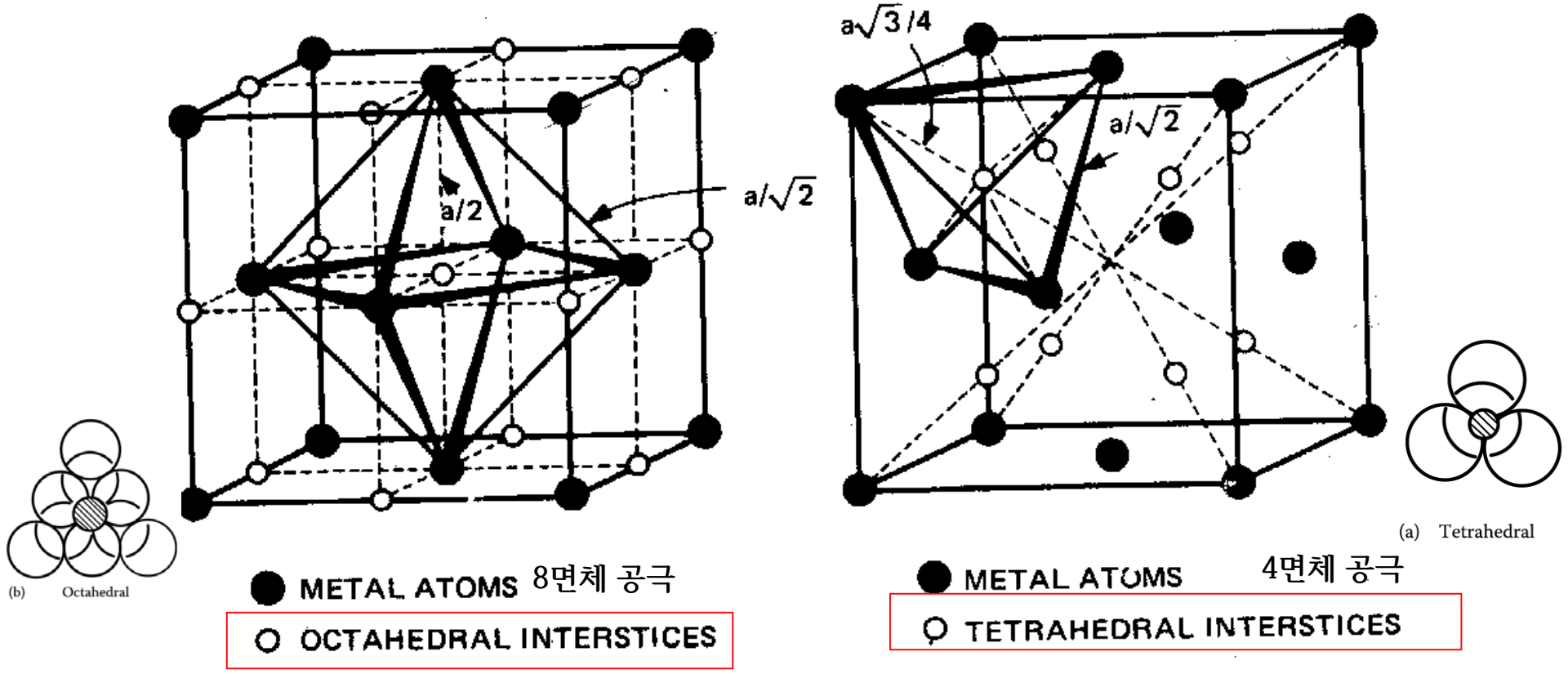

Six nearest neighbors/ d6 = 0.414D = 1.044 Å **surrounded by four atoms/ d4 = 0.225D = 0.568 Å**

D is the diameter of the parent atoms/ d4 and d6 are the maximum interstitial diameters

Diameter of a carbon atom: 1.54 Å

: This means that considerable distortion of the γ austnite lattice must occur to contain carbon atoms in solution and that the octahedral interstices should be the most favorable.

6.1.1 Solid Solution of carbon in Iron

Figure. Illustrating possible sites for interstitial atoms in the bcc lattices.

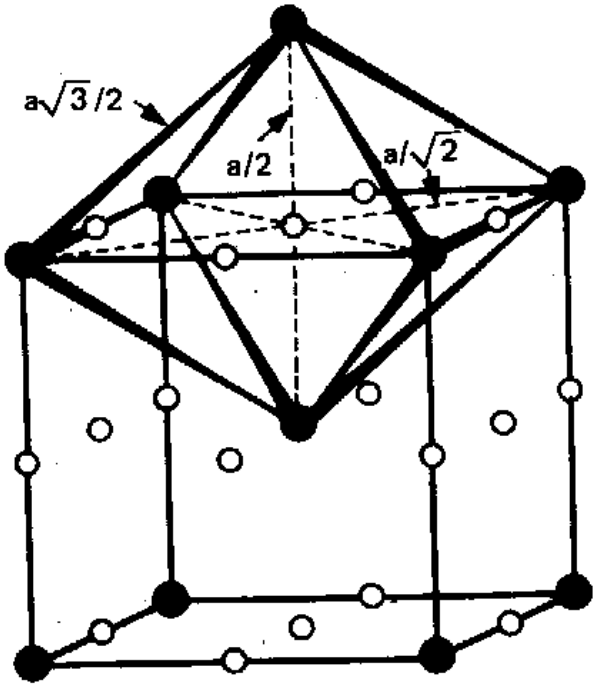

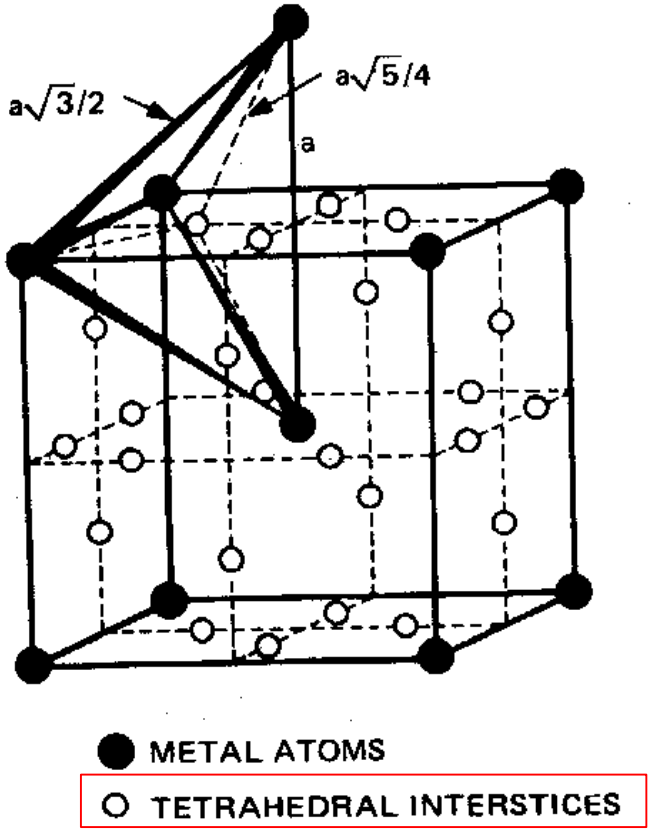

Three possible octahedral positions/
d6 = 0.155D = 0.391 Å

Six possible tetrahedral spaces/
d4 = 0.291D = 0.733 Å

D is the diameter of the parent atoms/ d4 and d6 are the maximum interstitial diameters

Free space: FCC < BCC but space available per interstitial: FCC > BCC

*** In spite of d6<d4, C & N prefer to occupy the octahedral positions in BCC.**

→ **required considerable distortion but <100> directions~weaker** due to the lower number of near and next nearest neighbors compared to the tetrahedral interstitial position

Interstitial sites
for C in Fe

fcc:
carbon occupies the octahedral sites

bcc:
carbon occupies the octahedral sites

[Leslie]

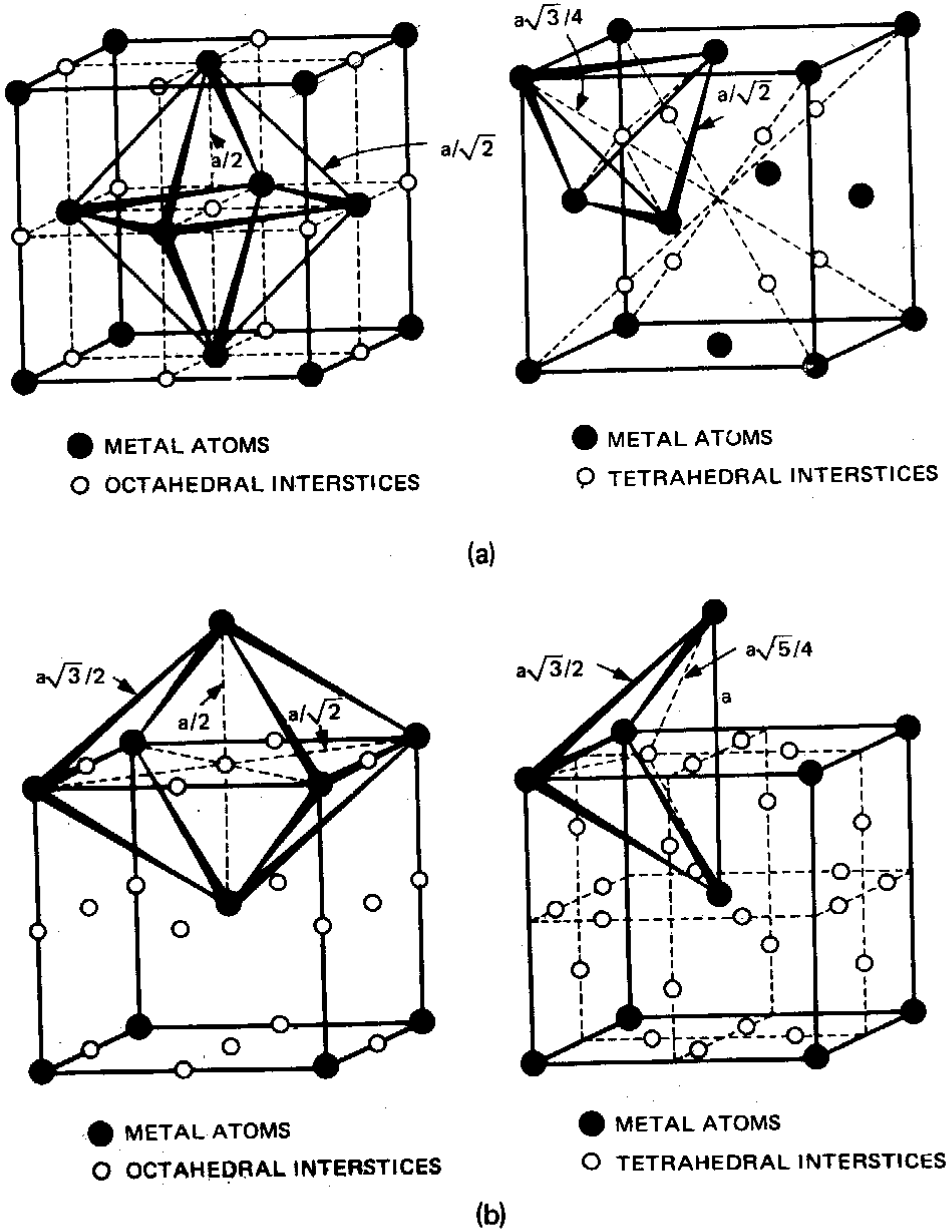

Figure II-1. Interstitial voids in iron. (*a*) Interstitial voids in the fcc structure, octahedral (1) and tetrahedral (2). (*b*) Interstitial voids in the bcc structure; octahedral (1) and tetrahedral (2). (From C.S. Barrett and T.B. Massalski, *Structure of Metals*, 3d ed., copyright 1966, used with the permission of McGraw-Hill Book Co., New York.)

Carbon in BCC α ferrite

[P&E]

- One consequence of the occupation of the octahedral site in ferrite is that the carbon atom has only two nearest neighbors.
- Each carbon atom therefore distorts the iron lattice in its vicinity.
- The distortion is a *tetragonal distortion*.
- If all the carbon atoms occupy the *same type of site* then the entire lattice becomes tetragonal, as in the martensitic structure.
- Switching of the carbon atom between adjacent sites leads to **strong internal friction peaks** at characteristic temperatures and frequencies.

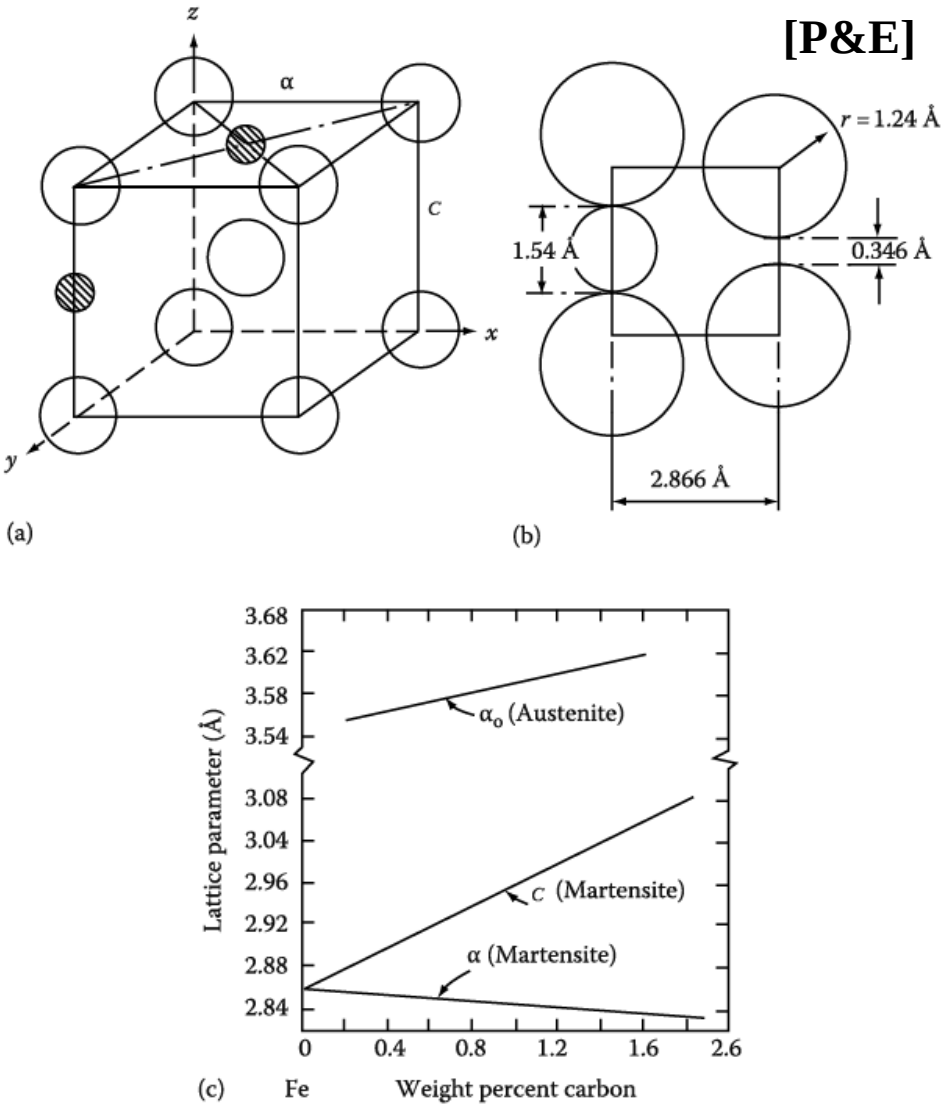

Fig. 6.5 Illustrating (a) possible sites for interstitial atoms in bcc lattice, and (b) the large distortion necessary to accommodate a carbon atom (1.54 Å diameter) compared with the space available (0.346 Å). (c) Variation of a and c as a function of carbon content.

Why tetragonal Fe-C martensite?

- At this point, it is worth stopping to ask why a tetragonal martensite forms in iron. The answer has to do with the preferred site for carbon as an interstitial impurity in bcc Fe.
- Remember: Fe-C martensites are unusual for being so strong (& brittle). Most martensites are not significantly stronger than their parent phases.
- Interstitial sites:
  fcc: octahedral sites radius= 0.052 nm
  tetrahedral sites radius= 0.028 nm
  bcc: octahedral sites radius= 0.019 nm
  tetrahedral sites radius= 0.036 nm
- Carbon atom radius = 0.08 nm.
- Surprisingly, it occupies the octahedral site in the bcc Fe structure, despite the smaller size of this site (compared to the tetrahedral sites) presumably because of the low modulus in the <100> directions.

6.2. Martensite crystallography (Orientation btw M & γ)

γ→α′: (1) Habit plane of M: not distorted by transformation

(2) A homogeneous shear (s) parallel to the habit plane

(3) ~4% expansion_dilatation normal to the habit plain (lens)

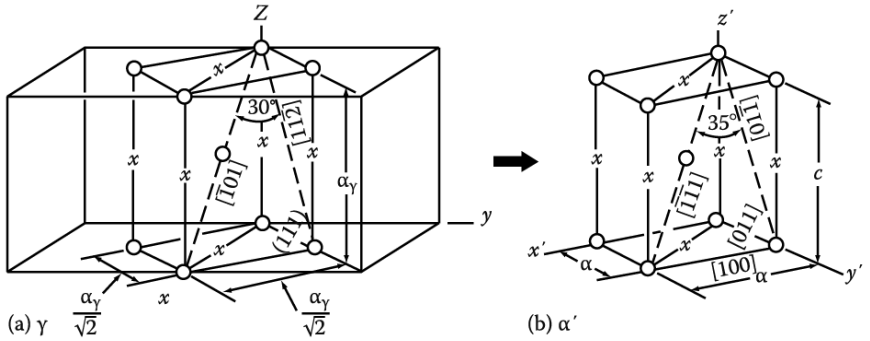

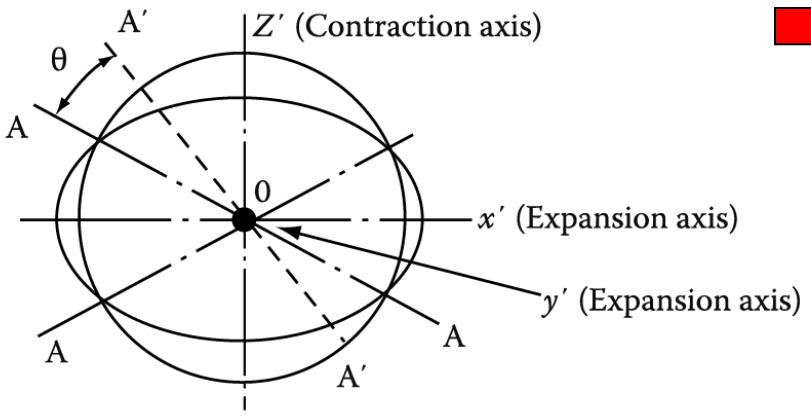

Bain Model for martensite

Applying the twinning analogy to the Bain model,

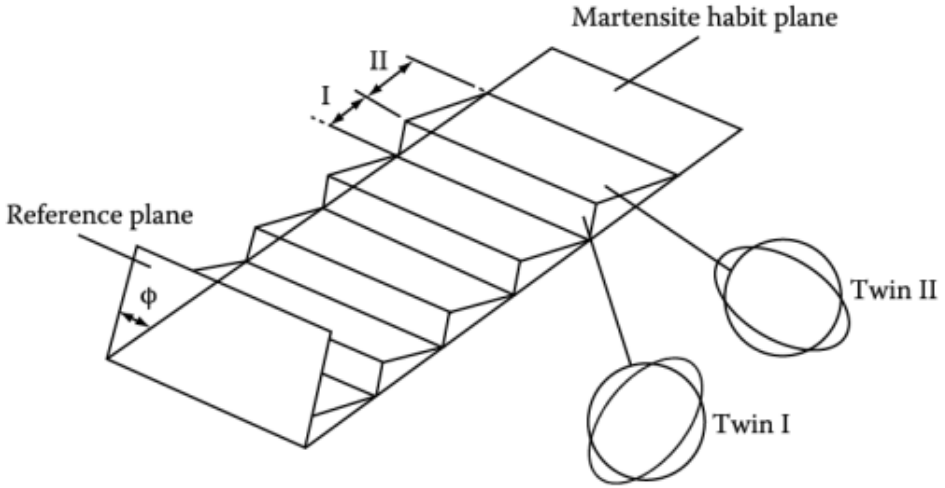

Twins in Martensite

may be self-accommodating and reduce energy by having alternate regions of the austenite undergo the Bain strain along different axes.

Possible atomic model for martensitic transformation:
the Bain Model: fcc → bct transformation

- For the case of FCC Fe transforming to BCT ferrite (Fe-C martensite), there is a basic model known as the Bain model.
- The essential point of the Bain model is that it accounts for the structural transformation with a *minimum of atomic motion*.
- Start with two FCC unit cells: contract by 20% in the z direction, and expand by 12% along the x and y directions.

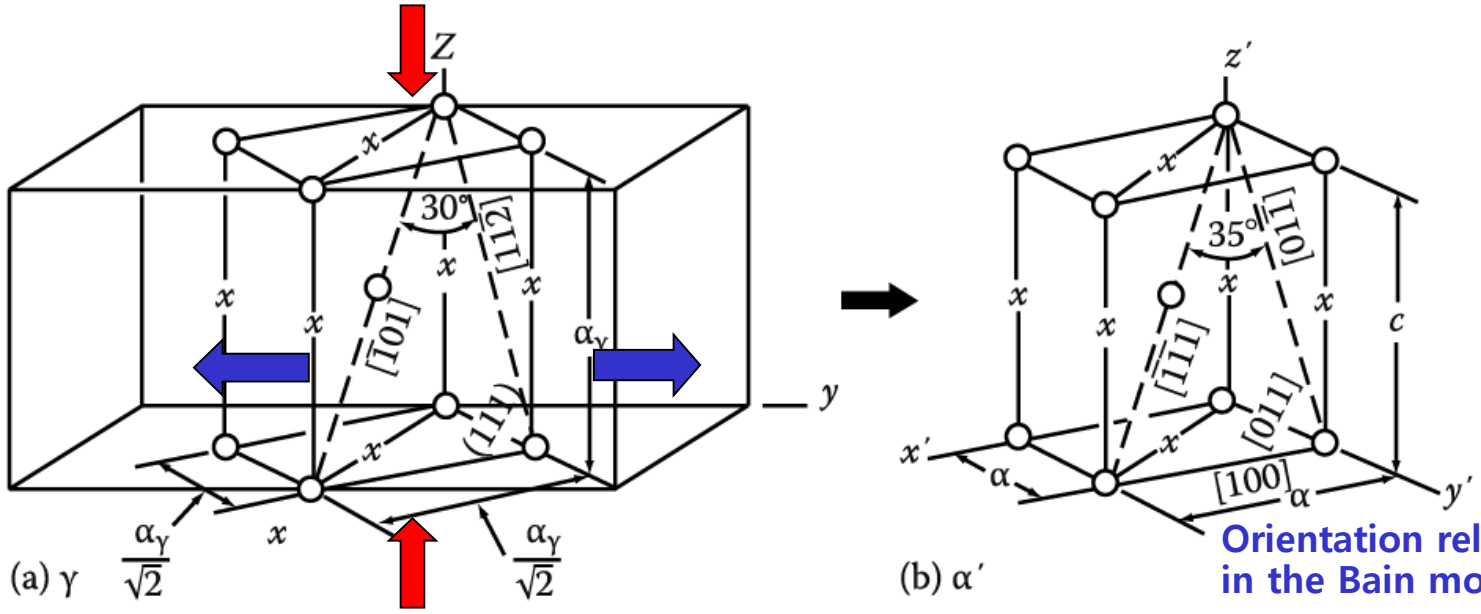

Orientation relationships in the Bain model are:

$(\bar{1}11)_\gamma \rightarrow (0\bar{1}1)_{\alpha'}$

$[\bar{1}01]_\gamma \rightarrow [\bar{1}\bar{1}1]_{\alpha'}$

$[1\bar{1}0]_\gamma \rightarrow [100]_{\alpha'}$

$[11\bar{2}]_\gamma \rightarrow [01\bar{1}]_{\alpha'}$

Figure. 6.7 Bain correspondence for the γ→α' transformation.
Possible interstitial sites for carbon are shown by crosses.

Crystallography, contd.

- Although the Bain model explains several basic aspects of martensite formation, additional features must be added for complete explanations (not discussed here).
- The missing component of the transformation strain is an additional shear that changes the character of the strain so that an invariant plane exists. This is explained in fig. 6.8.

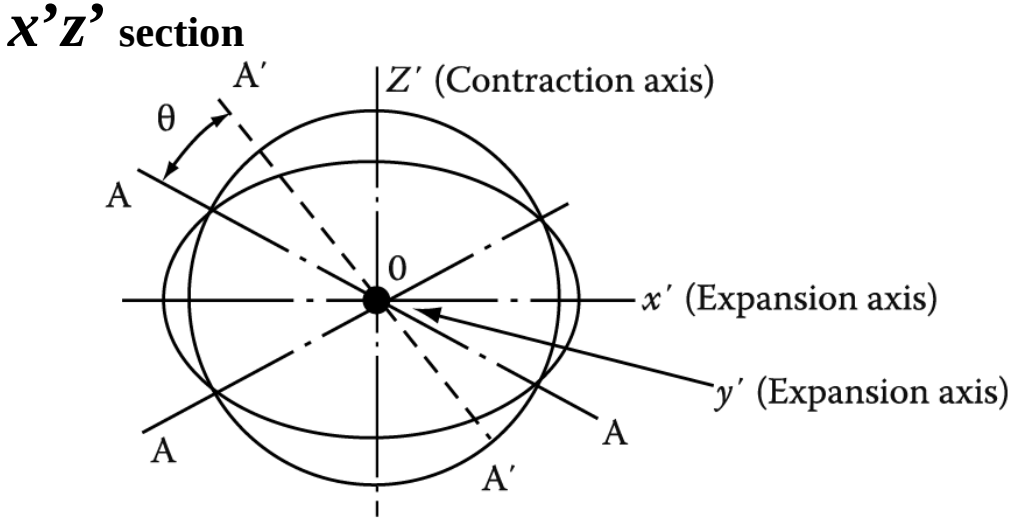

Fig. 6.8 Bain deformation is here simulated by the pure deformation in compressing a sphere elastically to the shape of an oblate ellipsoid. As in the bain deformation, this transformation involves two expansion axes and one contraction axis.

Bain deformation = Pure deformation

In this plane, the only vectors that are not shortened or elongated by the Bain distortion are OA or O'A'.

However, the vector OY' (perpendicular to the diagram) must be undistorted.

This is clearly not true and therefore the Bain transformation does not fulfill the requirements of bringing about a transformation with an undistorted plane. * 변형되지 않는 평면 설명 못함

Hence, the key to the crystallographic theory of martensitic transformations is to postulate an additional distortion which reduces the extension of y′ to zero (in fact a slight rotation, θ, of the AO plane should also be made as shown in the figure).

→ The second deformation can be in the form of dislocation slip or twinning.

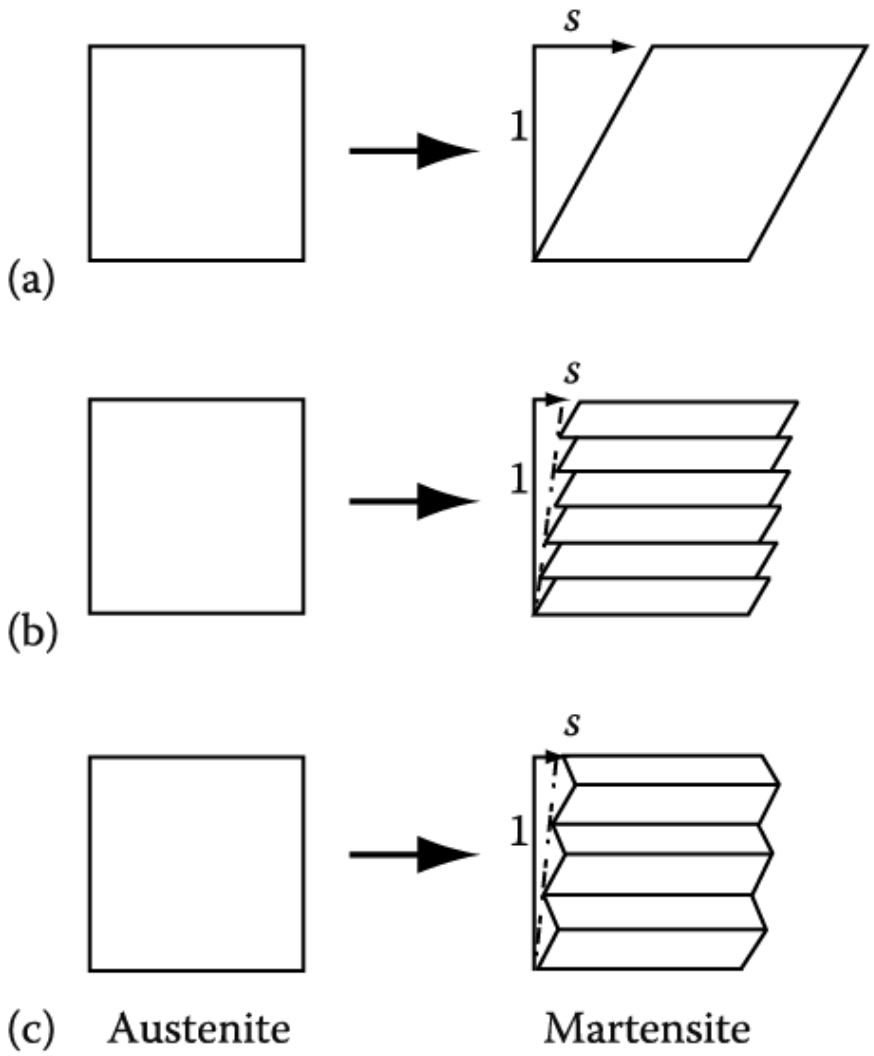

Figure. 6.9 Schematic illustration of how dislocation glide or twinning of the martensite can compensate for a pure lattice deformation such as a Bain deformation and thereby reduce the strain of the surrounding austenite. The transformation shear (s) is defined. Note how *S* can be reduced by slip or twinning.

Applying the twinning analogy to the Bain model,
the physical requirements of the theory are satisfied.

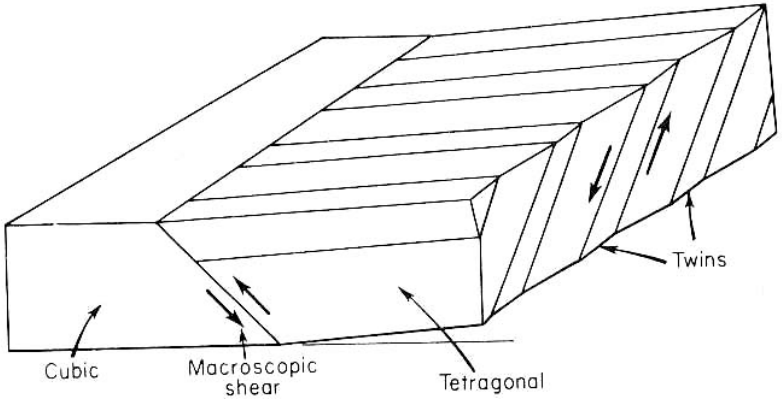

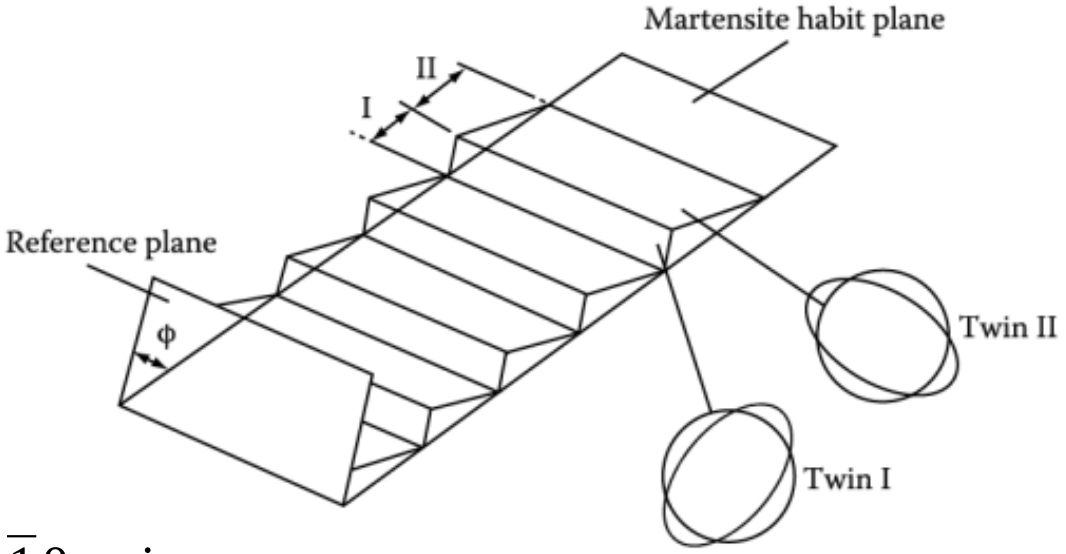

Slip or Twinning on

$$\{11\bar{2}\}<111> \text{ in } \alpha \quad \Leftrightarrow \quad \{110\}<1\bar{1}0> \text{ in } \gamma$$

BCC FCC

Twins in Martensite

may be self-accommodating and reduce energy by having alternate regions of the austenite undergo the Bain strain along different axes.

→ **On the basis, the habit plane of the M plate can be defined as a plane in the austenite which undergoes not net (macroscopic) distortion (=average distortion over many twins is zero)**

→ **Local strain E by twins at the edge of the plate, but if the plate is very thin (a few atomic spacings) this strain can be relatively small.**

6.2. Martensite crystallography (Orientation btw M & γ)

γ→α′: **(1) Habit plane of M: not distorted by transformation**

(2) A homogeneous shear (s) parallel to the habit plane

(3) ~4% expansion_dilatation normal to the habit plain (lens)

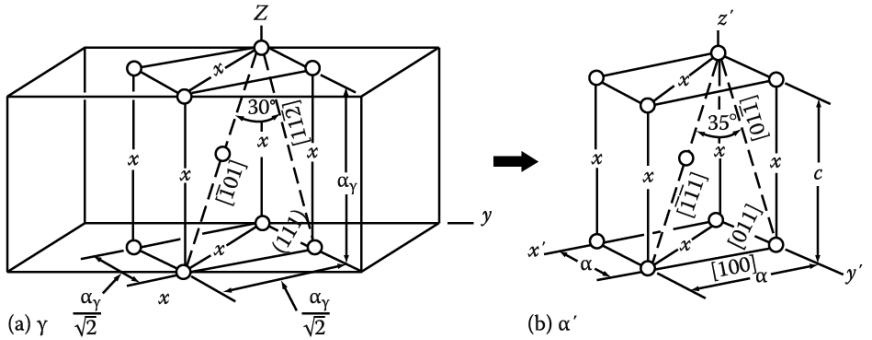

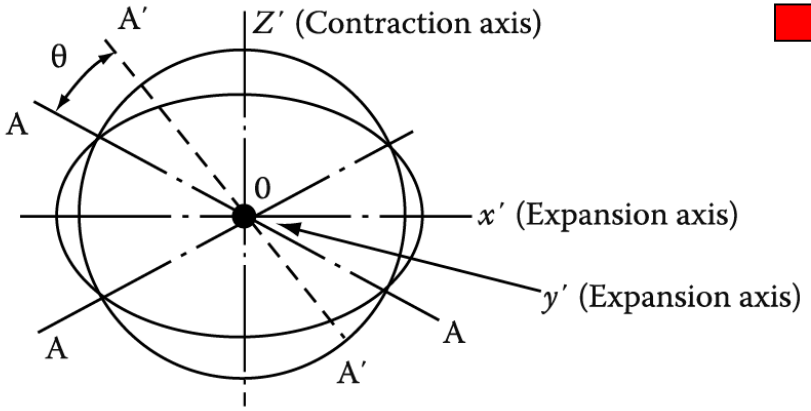

Bain Model for martensite

Applying the twinning analogy to the Bain model,

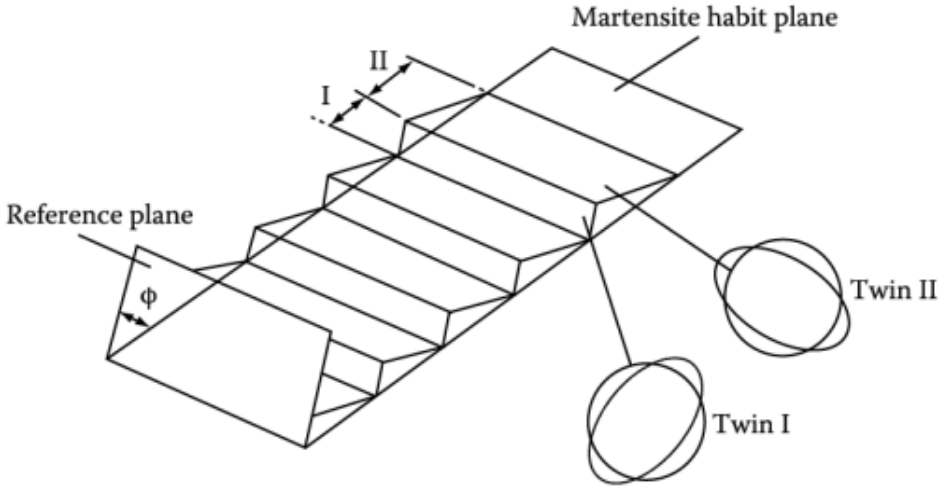

Twins in Martensite

may be self-accommodating and reduce energy by having alternate regions of the austenite undergo the Bain strain along different axes.

Q6:

Mechanisms for martensitic transformations?

- The mechanisms of military transformations are not entirely clear.

- **Why does martensite require heterogeneous nucleation?**
  The reason is the large critical free energy for nucleation outlined above

- Possible mechanisms for martensitic transformations include

  (a) dislocation based
  (b) shear based

(a)

- ***Dislocations*** **in the parent phase (austenite) clearly provide sites for heterogeneous nucleation.**
- **Dislocation mechanisms are thought to be important for *propagation/growth of martensite platelets or laths*.**

(b)

- Martensitic transformations strongly constrained by crystallography of the parent and product phases.
- This is analogous to slip (dislocation glide) and twinning, especially the latter.

6.3. Theories of Martensite Nucleation

Growth rate of single plate of M in steel: 10^{-5} to 10^{-7} s, ~the speed of sound

→ Using resistivity changes to monitor the growth of individual plates of M

e.g. Fe-Ni alloys: speed of 800-1100 m/s ~ difficult to study experimentally

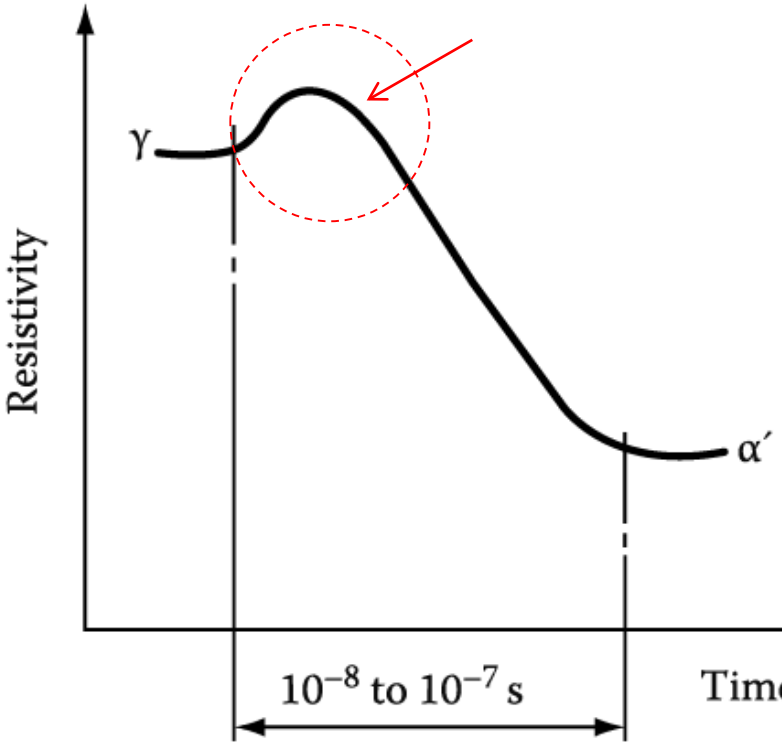

- **α′ gives lower resistivity than γ.**
- **Smaller initial increase in resistivity**

= initial strain of γ lattice by the M nucleus

= initial M nucleus ~ coherent with parent γ

Figure. 6.13 Resistivity changes during the growth of single plates of martensite across a grain in a Fe-Ni alloy. From this it can be calculated that the velocity of growth is about 1000 m/s.

6.3.1 Formation of Coherent Nuclei of Martensite (Homogenous nucleation)

Free Energy Change Associated with the Nucleation

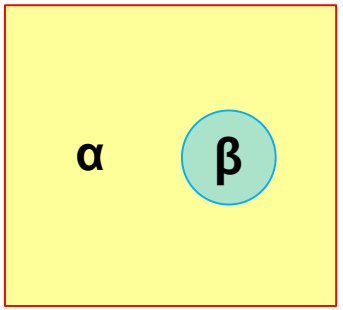

Negative and Positive Contributions to ΔG?

1) Volume Free Energy : $-V\Delta G_V$

2) Interface Energy : $A\gamma$

3) Misfit Strain Energy : $V\Delta G_S$

$$\Delta G = -V\Delta G_V + A\gamma + V\Delta G_S$$

This expression does not account for possible additional energies (e.g. thermal stresses during cooling, externally applied stresses, and stresses produced ahead of rapidly growing plates, etc).

In M transformations, the strain energy (ΔG_s) of the coherent nucleus is much more Important than the surface energy, since the shear component of the pure Bain strain is as high as S = 0.32 which produces large strains in the surrounding austenite. However, the interfacial (surface) energy (γ) of a fully coherent nucleus is relatively small.

(If homogenous nucleation) 6.3.1 Formation of Coherent Nuclei of Martensite

for thin ellipsoidal nucleus (radius a, semi thickness c and volume V),

$$\Delta G = A\gamma + V\Delta G_s - V\Delta G_v$$

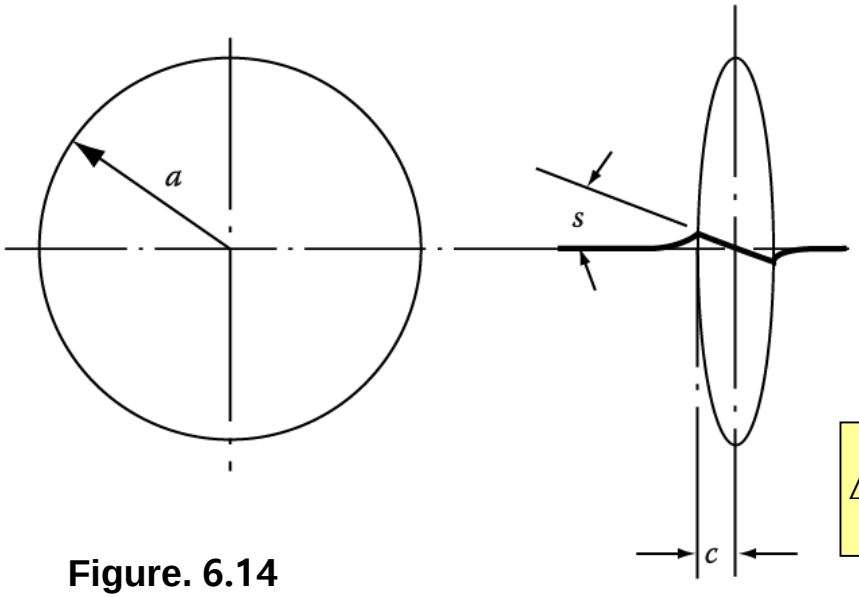

Figure. 6.14
Schematic representation of a M nucleus.

Assumption: 1) Nucleation does not necessarily occur at grain boundaries.
2) Nucleation occurs homogeneously without the aid of any other types of lattice defects.

→ The Nucleus forms by a simple shear, S, parallel to the plane of the disc, and complete coherency is maintained at the interface.

$$\Delta G = 2\pi a^2\gamma + 2\mu V(s/2)^2 \frac{2(2-\nu)}{8(1-\nu)}\pi c/a - \frac{4}{3}\pi a^2 c\cdot\Delta G_v$$

If ν=1/3,

$$\Delta G = 2\pi a^2\gamma + \frac{16\pi}{3}(s/2)^2\mu a c^2 - \frac{4\pi}{3}a^2 c\cdot\Delta G_v \qquad \text{Eq. (6.7)}$$

Surface E

Elastic E (shear component of strain only)

Volume E

6.3.1 Formation of Coherent Nuclei of Martensite

By differentiating Eq. (6.7) with respect to a and c, respectively

→ Min. free energy barrier to nucleation: extremely sensitive to "γ, ΔG_v and s"

$$\Delta G^* = \frac{512}{3} \cdot \frac{\gamma^3}{(\Delta G_v)^4} \cdot (s/2)^4 \mu^2 \pi$$ (joules/nucleus)

→ Critical nucleus size (c* and a*): highly dependent to "γ, ΔG_v and s"

$$c^* = \frac{2\gamma}{\Delta G_v} \qquad a^* = \frac{16\gamma\mu(s/2)^2}{(\Delta G_v)^2}$$ Eq. (6.9) & (6.10)

For steel, 1) typically $\Delta G_v = 174\ \mathrm{MJm^{-3}}$, and

2) s (varies according to whether the net shear of a whole plate (e.g. as measured from surface markings) or shear of fully coherent plate (as measured from lattice fringe micrographs)
= 0.2 (macroscopic shear strain in steel)

3) γ = 20 $\mathrm{mJm^{-2}}$ (fully coherent nucleus)

→ c*/a* ~ 1/40, ΔG* ~ 20 eV : <u>too high for thermal fluctuation alone to overcome</u> (at 700 K, kT = 0.06 eV)

→ "M nucleation = heterogeneous process" : possibly in dislocation
(#= 10^5 per 1 $\mathrm{mm^2}$)

6.3.2 Role of Dislocations in Martensite Nucleation
: based on ① atomic shuffles within the dislocation core

1) Zener: demonstrated how the movement of <112>$_\gamma$ partial dislocations during twinning could generate in thin bcc region of lattice from an fcc one.

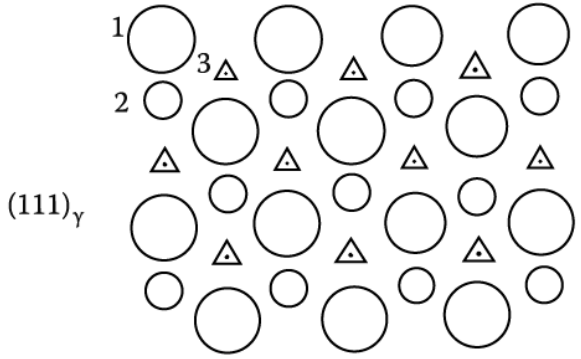

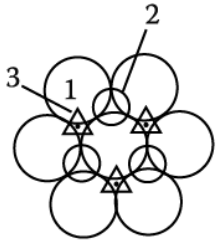

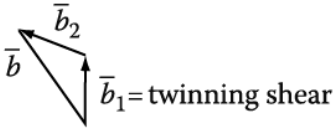

FCC
Close packed plane
1→3 = bottom to top layer

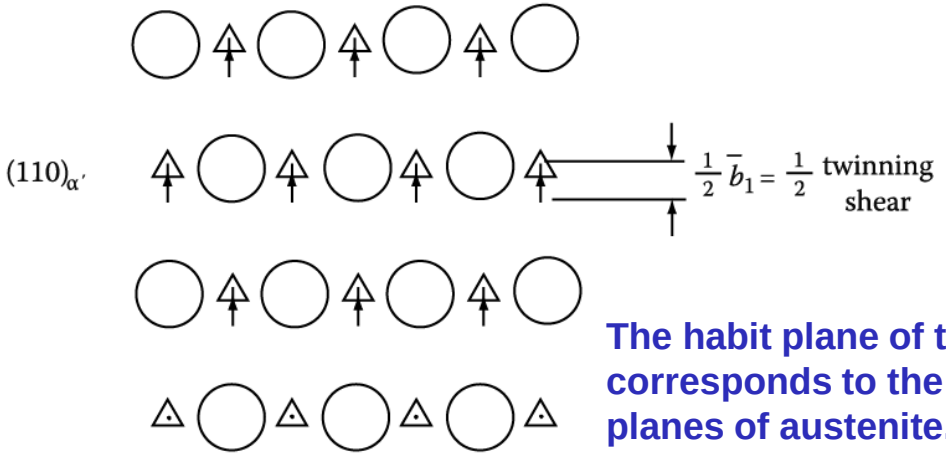

The habit plane of the M corresponds to the glide planes of austenite.

$$\bar{b} = \bar{b_1} + \bar{b_2}$$

$$\frac{a}{2}[\bar{1}10] = \frac{a}{6}[\bar{2}11] + \frac{a}{6}[\bar{1}2\bar{1}]$$

In order to generate the bcc structure it requires that all the 'triangular'
① (Level 3) atoms jumps forward by

$$\frac{1}{2}\bar{b_1} = \frac{a}{12}[\bar{2}11]$$

In fact, the lattice produced is only two atom layer thickness and not quite the bcc one after this shear, but requires an ② additional dilatation to bring about the correct lattice spacings.

Figure. 6.15 Zener's model of the generation of two-atom-thick martensite by a half-twinning shear (①+②)

Region with dislocation pile-ups
→ possible to form thicker M nuclei

6.3.2 Role of Dislocations in Martensite Nucleation

2) Venables: M transformation induced by half-twinning shear in fcc mater.

a. in the case of alloys of low stacking fault energy (e.g. steel, etc)

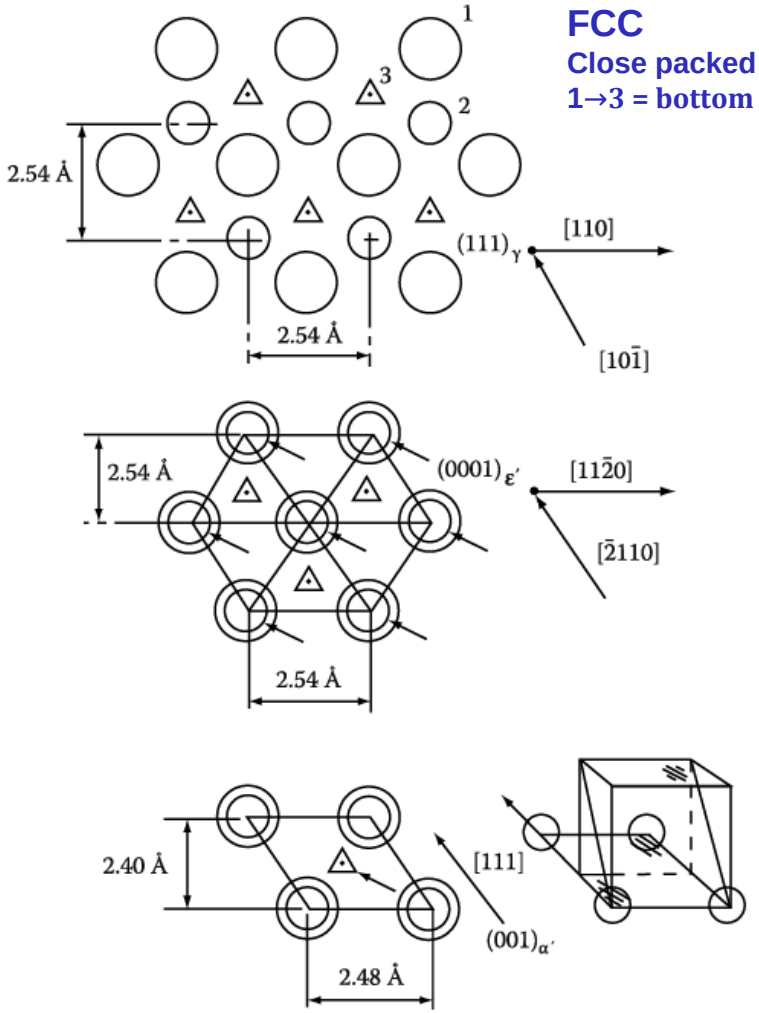

FCC
Close packed plane
1→3 = bottom to top layer

γ (fcc) → ε' (hcp) → α' (bcc)

ε'-martensite structure thickens by inhomogenous half-twining shears of on every other {111}γ plane. $\frac{a}{12}[\bar{2}11]$

→ **Indeed, α' regions have been observed to form in conjunction with M.**

→ **But, no direct evidence of the ε'→α' transition**

→ **possible γ→ε' and γ→α' by different mechanism**

Figure. 6.16 Venables's model for the γ→ε'→α'

6.3.2 Role of Dislocations in Martensite Nucleation

2) Venables: M transformation induced by half-twinning shear in fcc mater.

b. (example) **M transformation in Co** : **i) fcc → hcp transformation at around 390 °C**

habit plane {111}γ Orientation relationship (111)γ//(0001)α' → Generation of large number of

$\frac{a}{6}<11\bar{2}>_{\gamma}$ partial dislocations

on {111}γ plane → G.B. initiation

of stacking fault

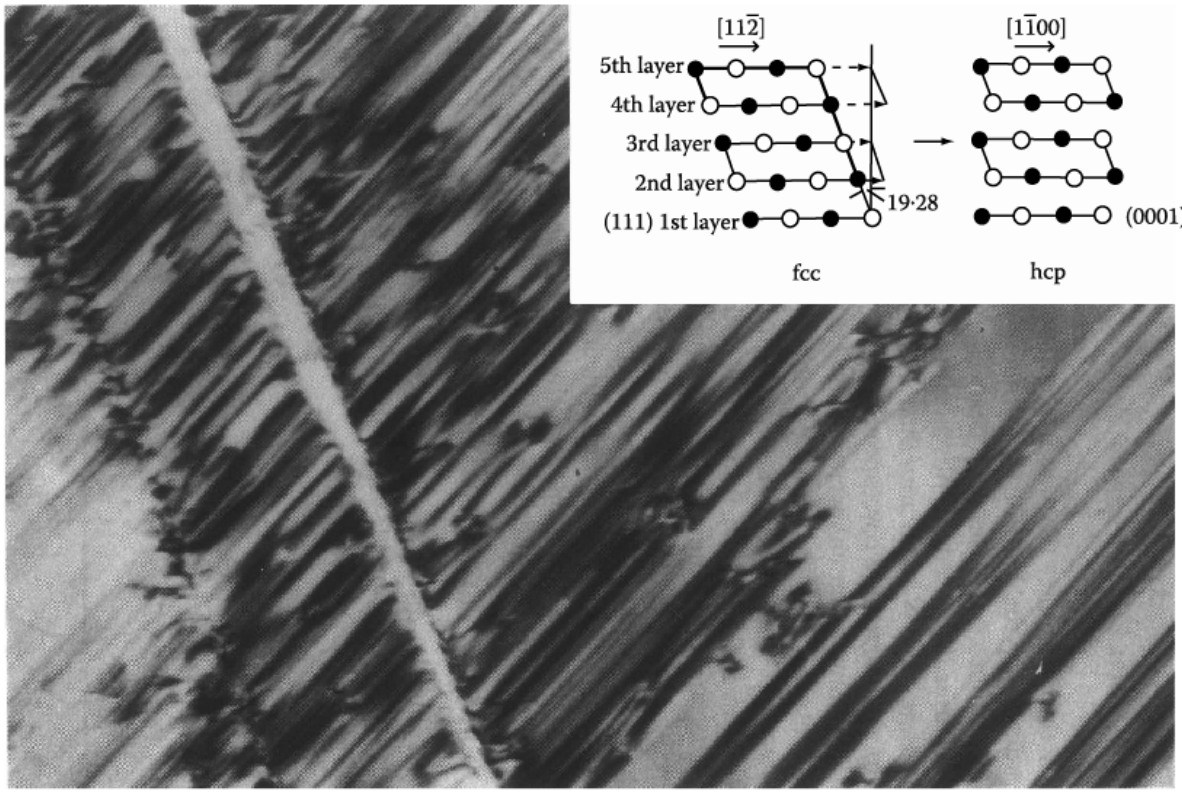

In-situ heating in TEM

ii) hcp → fcc reaction at 430 °C

Dissociation of dislocation on the hcp basal plane:

$$\frac{1}{3}[\bar{1}2\bar{1}0] \rightarrow \frac{1}{3}[01\bar{1}0] + \frac{1}{3}[\bar{1}100]$$

The reaction has to occur on every other hcp plane in order to generate the fcc structure

Figure. 6.18 Dislocation-assisted M transformation in cobalt. The insert illustrates the way stacking fault formation induces the fcc → hcp transformation.

6.3.2 Role of Dislocations in Martensite Nucleation

Understanding so far…

- **It is thus seen that some types of M can form directly by the systematic generation and movement of extended dislocations.**

  (M transformation induced by half-twinning shear in fcc mater related to ① atomic shuffles within the dislocation core)

  → M_s temperature : a transition from positive to negative SFE

Limitation…

- **However, 1) this transition type cannot occur in ① high SFE nor in ② thermoelastic martensites**

  2) this transition is also difficult to understand ③ twinned martensite, merely on the basis of dislocation core changes.

→ need to consider alternative way in which dislocations can nucleate martensite other than by changes at their cores.

6.3.3 ② Dislocation strain energy assisted transformation : help of the elastic strain field of a dislocation for M nucleation

- **Assumption: coherent nuclei are generated by a pure Bain strain, as in the classical theories of nucleation**

The stain field associated with a dislocation can in certain cases provide a favorable interaction with the strain field of the martensite nucleus, such that one of the components of the Bain strain is neutralized thereby reducing the total energy of nucleation.

→ the dilatation associated with the a)extra half plane of the dislocation contributes to the Bain strain.

→ Alternatively, the shear component of the dislocation could be utilized for M transformation.

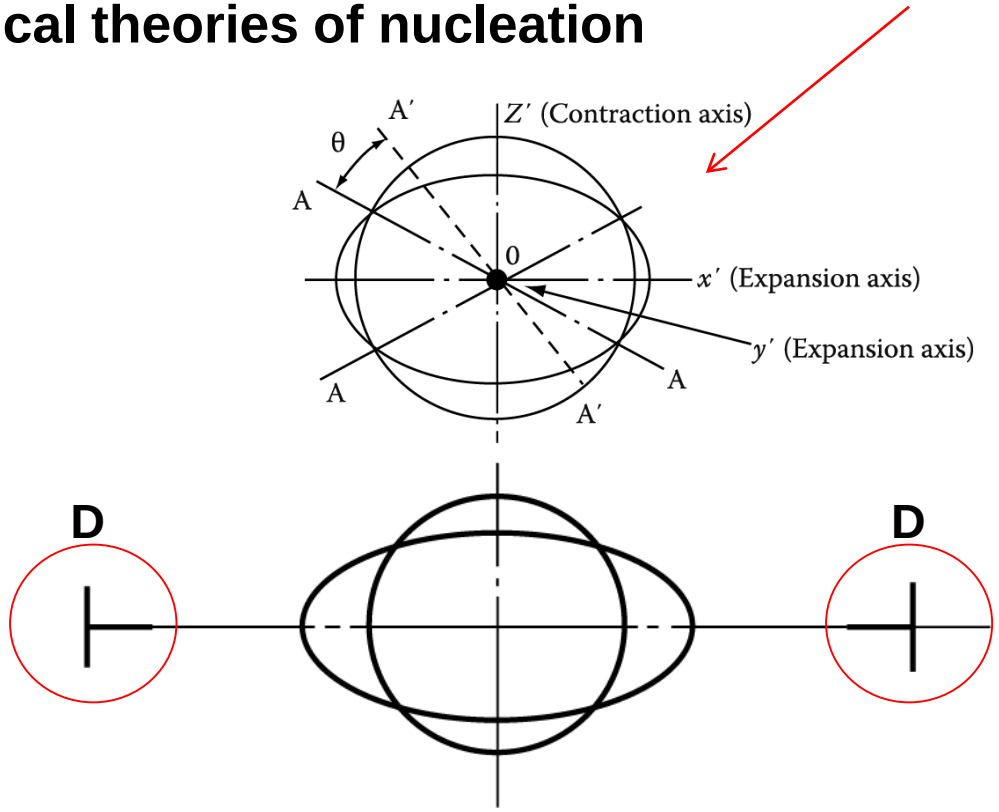

Figure. 6.19 Illustrating how one of the strain components of the Bain deformation may be compensated for by the strain field of a dislocation which in this case is tending to push atom planes together.

6.3.3 ② Dislocation strain energy assisted transformation
: help of the elastic strain field of a dislocation for M nucleation

$$\Delta G = A\gamma + V\Delta G_s - V\Delta G_v - \Delta G_d$$

Creation of nucleus~destruction of a defect($-\Delta G_d$)
→ Dislocation interaction energy which reduces the nucleation energy barrier

$$\Delta G_d = 2\mu s\pi \cdot ac \cdot \bar{b}$$

where $\bar{b}$ = Burgers vector of the dislocation,
s = shear strain of the nucleus

$$\Delta G = 2\pi a^2\gamma + \frac{16\pi}{3}(s/2)^2 \mu ac^2 - \frac{4\pi}{3}a^2 c \cdot \Delta G_v - 2\mu s\pi ac \cdot \bar{b}$$ Eq. (6.16)

전단변형과 bain 변형 포함

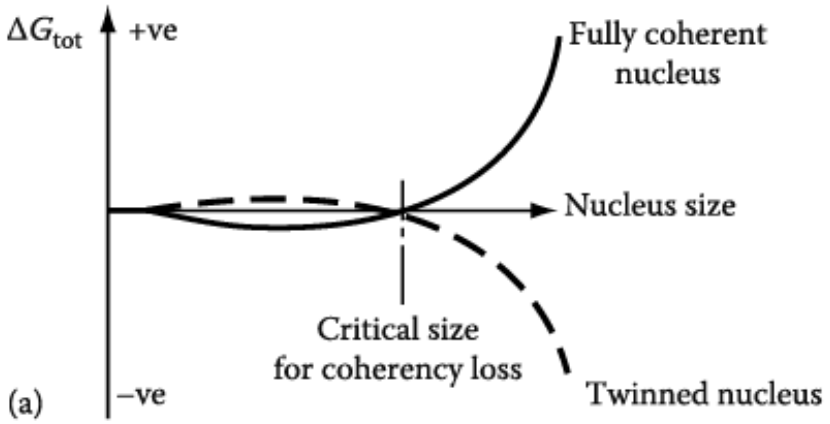

Figure. 6.20 (a) schematic diagram based on Eq. 6.16, illustrating the need for the nucleus to twin if it is to grow beyond a certain critical size.

→ **Total energy of martensite nucleus:**
as a function of 1) diameter and thickness (a, c)
(whether it is twinned or not (this affect "*s*"))
2) Degree of assistance from the strain field of a dislocation (or group of dislocations)

e.g. A fully coherent nucleus from partial interaction with the strain field of a dislocation ~ 20 nm dia. & 2-3 atoms in thickness → further growth need to twin and slip formation

6.3.3 ② Dislocation strain energy assisted transformation
: help of the elastic strain field of a dislocation for M nucleation

Burst phenomenon

: auto-catalytic process of rapid, successive M plate formation occurs over a small temperature range , e.g. Fe-Ni alloys
(Large elastic stresses set up ahead of a growing M plate → Elastic strain field of the M plate act as the interaction term of elastic strain field of dislocation in Eq. (6.16) → reduces the M nucleation energy barrier)

In summary,

- **we have not dealt with all the theories of martensite nucleation in this section as recorded in the literature, or even with all alloys exhibiting martensitic transformations.**

- **Instead we have attempted to "illustrate some of the difficulties associated with explaining a complex event which occurs at such great speeds as to exclude experimental observation."**

- **A general, all embracing theory of martensite nucleation has still evaded us, and may not even be feasible.**